INVESTIGATION OF THE STRUCTURAL BEHAVIOR OF ASPHALT/WOOD DECK SYSTEMS FOR GIRDER BRIDGES

Joseph N. Howard

Thesis submitted to the Faculty of the Virginia Polytechnic Institute and State University
in partial fulfillment of the requirements for the degree of

Master of Science
in
Civil Engineering

J. Daniel Dolan, Co-Chairman
Joseph R. Loferski, Co-Chairman
Richard E. Weyers

April, 1997
Blacksburg, Virginia

Keywords: Timber Bridge, Glulam Bridge, Deck Deflection

INVESTIGATION OF THE STRUCTURAL BEHAVIOR OF ASPHALT/WOOD DECK SYSTEMS FOR GIRDER BRIDGES

(ABSTRACT)

Glue laminated wood deck systems are commonly used for bridge decks on girder bridge systems. These decks are usually covered with a hot-mix asphalt wearing surface in conjunction with a bituminized fabric sheet waterproofing membrane. Often cracks occur in the asphalt at the intersection of two adjacent deck panels which limits the useful life of the wear surface, provides a poor riding surface and potentially allows moisture to flow to wooden bridge components.

The purpose of this study was to investigate the structural behavior of asphalt/wood/membrane deck systems. This was accomplished experimentally by determining the deflection of bridge deck panels with respect to each other under simulated truck loading. A classical linear analysis model and a finite element analysis model were developed for the deck panel deflections. These analytical results were compared to the experimental results and a value of approximately 0.05 in for the interpanel differential deflection was determined to be a reasonable, conservative value for the typical configuration considered. This deflection was then used to load various asphalt/membrane/wood configurations to investigate the effectiveness of the arrangement with regards to resisting hot-mix asphalt cracking. It was found that when subjected to repeated deflections of 0.05 in, the following experimental composite bridge deck performed best in terms of reduced cracking: 1) hot-mix asphalt base layer applied directly onto the glulam deck panel; 2) waterproofing membrane placed on the base layer of asphalt; 3) hot-mix asphalt surface layer placed on the waterproofing membrane.

ACKNOWLEDGMENTS

The author wishes to express his sincere gratitude to Professors J. Daniel Dolan, Joseph R. Loferski and Richard E. Weyers for their direction and advice as committee members. Thanks goes to Professor Thomas M. Murray for instruction in the art of setting and attaining goals. A great deal of thanks goes out to John Haramis for his invaluable assistance with the experimental testing. Special thanks go out to the United States Department of Agriculture Forest Products Lab for sponsoring this research through Research Contract No. FP-94-2272. Finally, the author would like to thank his loving wife, Athena, for her support and encouragement throughout this endeavor and his children, Tom, Elizabeth, and Astraea for sharing their dad with this study.

TABLE OF CONTENTS

ABSTRACT ii

ACKNOWLEDGEMENTS iii

TABLE OF CONTENTS iv

LIST OF FIGURES vii

LIST OF TABLES viii

CHAPTER I. INTRODUCTION

1.1 GENERAL 1

1.2 LITERATURE REVIEW 4

1.2.1 Glue Laminated Girder Bridges 4

1.2.2 Asphalt Pavement Wearing Surfaces 6

1.2.3 Finite Element Modeling of Timber Bridge Decks 7

1.3 SCOPE AND PURPOSE OF RESEARCH 8

CHAPTER II. ANALYTICAL INVESTIGATION OF GLULAM DECK PANELS

2.1 GENERAL 9

2.2 DEFLECTION ANALYSIS DETAILS 9

2.2.1 Member Geometry and Assumptions 9

2.2.2 Classical Method 10

2.2.3 Finite Element Method 18

2.3 DEFLECTION ANALYSIS RESULTS 19

CHAPTER III. EXPERIMENTAL INVESTIGATION OF GLULAM DECK PANELS AND WEARING SURFACE OVERLAYS

3.1 SCOPE OF TESTING 27

3.1.1 Interpanel Deck Deflection 27
3.1.2 Asphalt Crack Promulgation 27
2.2 DEFLECTION TEST DETAILS 29
3.2.1 Deflection Test Specimens 29
3.2.2 Deflection Test Setup 29
3.2.3 Deflection Test Instrumentation 29
3.2.4 Deflection Test Procedure 34
3.3 DEFLECTION TEST RESULTS 34
3.4 CRACKING TEST DETAILS 34
3.4.1 Cracking Test Specimens 34
3.4.2 Cracking Test Setup 35
3.4.3 Cracking Test Instrumentation 35
3.4.4 Cracking Test Procedure 37
3.5 CRACKING TEST RESULTS 37

CHAPTER IV. ANALYTICAL AND EXPERIMENTAL RESULTS
4.1 INTERPANEL DECK DEFLECTIONS 44
4.2 ASPHALT/WOOD BEHAVIOR 50

CHAPTER V. PROPOSED DESIGN METHOD
5.1 BACKGROUND 52
5.2 PROPOSED DECK DEFLECTION MODEL 52
5.3 LIMITATIONS 54

CHAPTER VI. CONCLUSIONS
6.1 OBSERVATIONS 55
6.2 RECOMMENDATIONS 55
6.3 FUTURE RESEARCH NEEDS 56

REFERENCES 57

APPENDIX A TEST SUMMARY SHEETS..... 58

APPENDIX B FINITE ELEMENT INPUT FILE LISTINGS 92

APPENDIX C SAMPLE INTERPANEL DIFFERENTIAL DEFLECTION CALCULATION 98

VITA 101

LIST OF FIGURES

Figure		Page
1.1	Typical Longitudinal Deck Bridge	3
1.2	Typical Glued Laminated Girder Bridge	7
2.1	Panel Loading Configuration	10
2.2	Simple Beam Analysis Configuration	12
2.3	Simple Beam - Load vs. Deflection Plot	13
2.4	Continuous Beam Analysis Configuration	16
2.5	Continuous Beam - Load vs. Deflection Plot	20
2.6	Finite Element Model Configurations	22
2.7	Simple Beam - Classical and Finite Element Comparison	25
2.8	Continuous Beam - Classical and Finite Element Comparison	26
3.1	Typical Deflection Test Configuration	28
3.2	Typical Asphalt Cracking Test Configuration	30
3.3	Deflection Test Boundary Conditions	32
3.4	Deflection Instrumentation Location	33
3.5	Experimental Load vs. Deflection Plot - Simple Beam	38
3.6	Experimental Load vs. Deflection - Continuous Beam	39
3.7	Cracking Test Instrumentation Location	42
4.1	Experimental Load vs. Deflection with Confidence Intervals for Simple Beams	45
4.2	Experimental Load vs. Deflection with Confidence Intervals for Continuous Beams	46

LIST OF TABLES

Table		Page
2.1	Flexural and Shear Deformation Comparison	21
2.2	Classical and Finite Element Model Results (5-1/8 in.)	23
2.3	Classical and Finite Element Model Results (6-3/4 in.)	24
3.1	Deflection Test Matrix	31
3.2	Comparative Deflection Test Summary	36
3.3	Asphalt Content and Gradation of Test Mixtures	40
3.4	Cracking Test Matrix	41
3.5	Cracking Test Summary	43
4.1	Comparative Experimental Results	47
4.2	Average Modulus of Elasticity Results	47
4.3	Specific Modulus of Elasticity Results	48
4.4	Comparative Deflections for Experimental Continuous Configuration	49
4.5	Configuration of Uncracked Test Specimens	51

CHAPTER I

INTRODUCTION

1.1 GENERAL

Timber bridges are becoming more prevalent as new bridges are constructed for short to medium spans. The first bridges constructed by mankind were probably wood structures. Some of the earliest recorded wood bridge designs were promulgated in the 16th century by the Venetian engineer, Palladio, but timber bridges were not constructed in earnest until the 18th century in Europe and at the beginning of 19th century in America. Steel and concrete have been the predominate construction material for bridges since the early 1900's but there has been a dramatic increase in the number of new timber bridges constructed in the latter portion of the 20th century. Timber bridges have some inherent advantages which have instigated this resurgence of interest.

One of the main advantages of timber bridges over steel or concrete is speed of construction. This is very important on high volume or critical use roads. Timber is a renewable resource and timber bridge structures are aesthetically pleasing. Timber bridges can be constructed in all types of weather and climates, including wet and cold conditions. Timber bridges can withstand dynamic loading well and are not as susceptible to fatigue crack growth as those constructed with other materials. Timber is relatively light which allows the use of smaller equipment for erection and therefore reduces construction costs. Wood bridge members are not significantly affected by salt and other deicing agents, although the metal fasteners used in timber bridges may be affected.

Timber bridges do have some disadvantages compared to other construction materials. Wood is an organic material and is susceptible to damage by fungi, insects, marine borers, fire and wear. The fungal damage will occur only when the moisture content of the wood approaches or is greater than the fiber saturation point of around twenty percent. Chemical preservation of wood is used to prevent or retard damage by fungi, insects, marine borers and fire. A protecting surface, such as asphalt, is applied to timber bridge decks to prevent wearing. Attention must be given to avoid excess moisture buildup between the timber elements and the wearing surface. Futhermore, deflections of the timber deck must be limited to prevent premature cracking of the asphalt surface, a common problem with many timber bridges. These cracks are probably caused by the deflection of one timber deck panel with respect to an adjacent timber deck panel. This phenomenom is called interpanel differential deck deflection.

There are three major types of timber bridges; longitudinal girder superstructures, longitudinal deck superstructures, and trusses as presented by Ritter (1992). Longitudinal girder superstructures consist of transverse wooden decks supported by longitudinal beams spanning two or more supports (abutments or piers). Modern highway timber bridge girders are usually glued laminated timber (glulam), laminated veneer lumber (LVL), or steel W shapes and are typically used in spans from 20 ft to 80 ft. The decks on timber girder bridges are almost always glue laminated and usually are 4 ft wide and 24 ft to 30 ft long. Longitudinal girder superstructures are discussed in detail in Section 1.2.1.

Williamson (1990) describes longitudinal deck bridges as a system where the glulam deck panels are placed longitudinal to the bridge span and thus eliminate the need for girders. This system is intended for shorter span applications up to approximately system is very useful where a bridge with a high clearance and a low profile is desired. In order to distribute loads across adjacent deck panels and limit interpanel deflections, spreader (or needle) beams are used. The spreader beams are usually glulam sections bolted to the deck panels. An example of a longitudinal deck bridge is shown in Figure 1.1. An alternative type of longitudinal deck bridge is the stress-lam bridge. This type of bridge is similar in geometry but the method of laminating the deck panels is different. The stress-lam relies on the friction created by passing stressing rods through the wide face of the individual deck lamina to transfer and distribute the bridge loads in a method similar to a glulam deck panel.

A timber truss is a structural frame combination of small straight wooden members connected to form a planar series of triangles. The nostalgic covered bridges used this type of superstructure to span upwards of one-hundred-fifty feet but required very deep truss structures. Dimakis *et al* (1988) relate a new idea for short span bridges borrowed from recent technology developed for light frame construction. A parallel chord bridge could be made from trusses fabricated primarily from dimensional lumber rather than glulam or larger timbers. The adjacent trusses would be in contact much like the elements in a longitudinal deck. The resulting system forms a wooden box girder extending the length of the span and acting similarly to a concrete box girder bridge.

Other types of timber bridges are log beam superstructures, sawn lumber superstructures, trestles, glulam arch bridges, and suspension bridges but these types of bridges have limited use for modern highway bridges. The longitudinal girder superstructure, longitudinal deck superstructure, and truss bridges are the most prevalent designs being constructed for modern highway bridges today. Since new timber bridges are currently being constructed, it is necessary to try to ensure longevity of these structures.

Current deck deflection design practice as described by Ritter (1992) is to check the thickness of the deck and the span between girders against a chart derived from

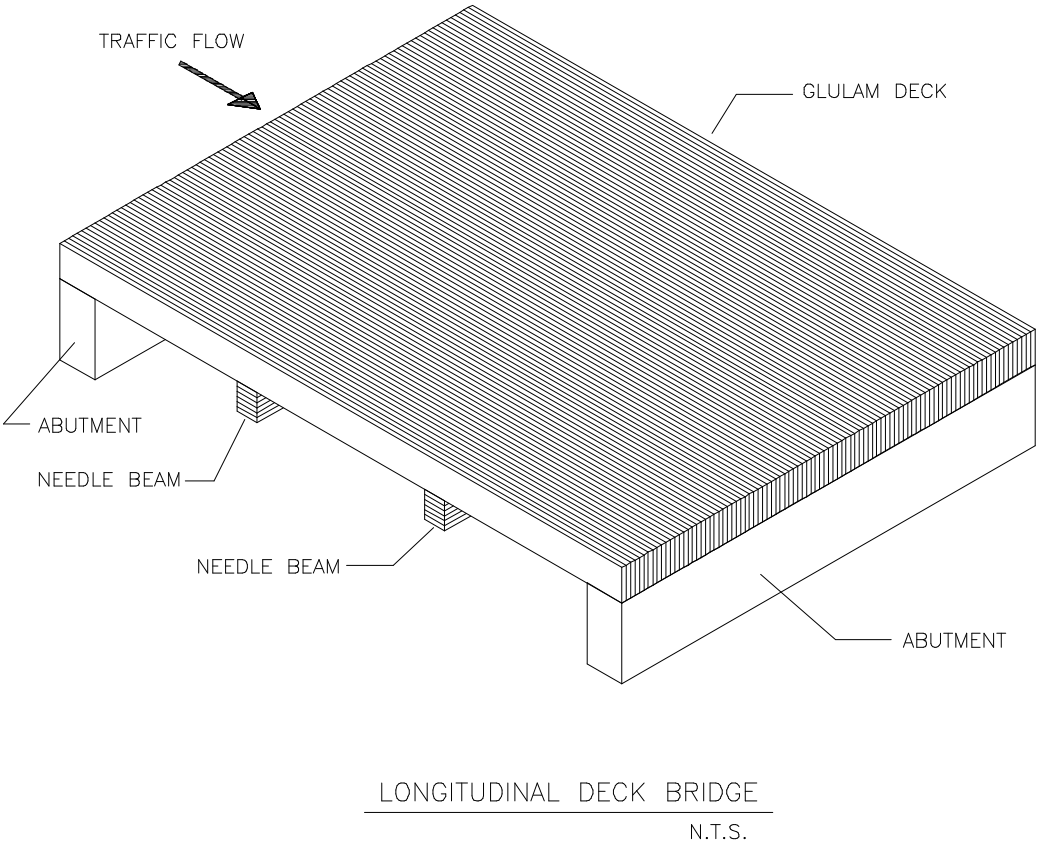

Figure 1.1 Longitudinal Deck Bridge

research and field observations for noninterconnected decks. This study was sponsored by the United States Department of Agriculture Forest Products Lab in Madison, Wisconsin and quantified the allowable deflections and design criteria for interpanel deck deflections. The objective of this study was: 1) experimentally quantify classical and finite element models of interpanel deck deflections (decks considered were glued laminated wood deck panels, the most commonly used timber deck, the structure considered was the girder, or stringer type of bridge superstructure); 2) experimentally investigate the performance of specific asphalt/wood configurations with regards to cracking under cyclic loading of a prescribed displacement.

1.2 LITERATURE REVIEW

1.2.1 GLUED LAMINATED GIRDER BRIDGE DECKS

Glued laminated girder bridges consist of transverse glulam deck panels supported by longitudinal glued laminated girders which span from abutment to abutment (or pier). An example of a glulam girder bridge with a glulam deck is shown in Figure 1.2. Girders are the principal load carrying components of the bridge superstructure and the deck panels distribute the load to the girders. Girders are designed to resist the applied loads and meet the deflection requirements for serviceability. They are usually designed with lateral bracing for stability concerns and must withstand the bearing loads. Glued laminated girder bridges can be used economically on spans up to about 80 ft. Ritter (1992) presents the design of glulam beams and beam components as well as glulam decks.

Williamson (1990) describes glue laminated timber as an assembly of individual dimensional wood laminations bonded together such that the grain of all pieces is produced in virtually any size by end joining the individual lamina and then bonding the wide face of the laminae with a waterproof structural adhesive. Glulam timbers are produced in approximately thirty manufacturing facilities throughout the United States. The lamina can be selectively placed in the glulam member so that the highest quality laminae are placed in the areas subjected to the highest stress. Glulam timbers can be manufactured from both softwood and hardwood lumber and are stress rated in accordance with the American National Standard for Wood Products-Structural Glued Laminated Timber, ANSI/AITC A190.1.

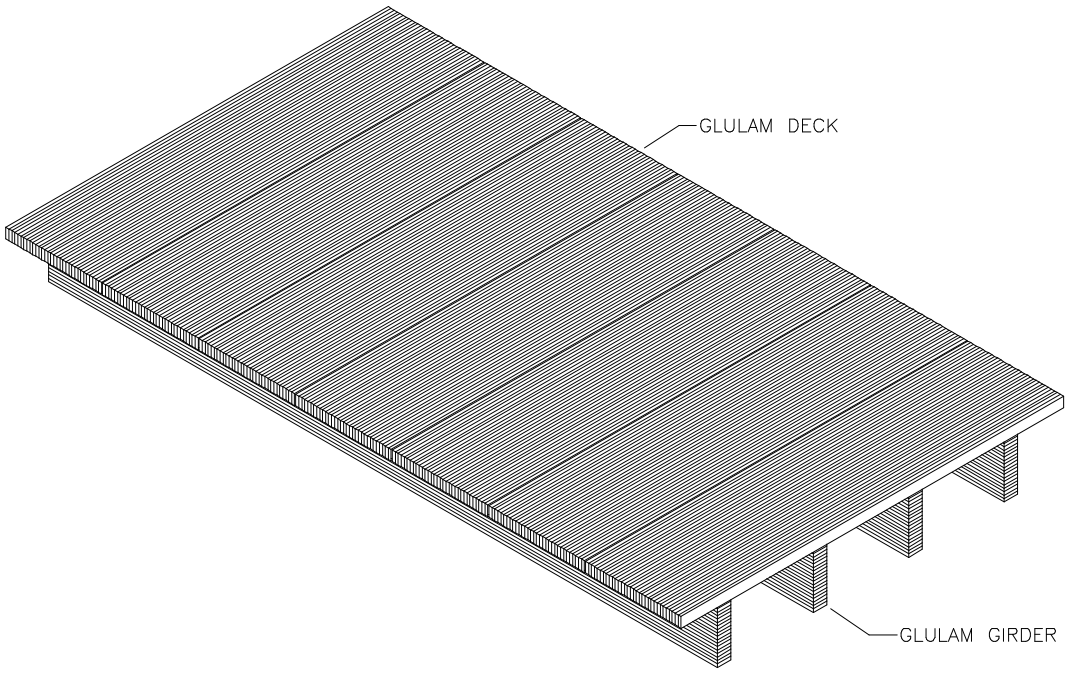

Figure 1.2 Glulam Girder Bridge

Gutkowski *et al* (1983) reported that the United States Forest Products Lab initiated a research program in the late 1960's to investigate glued laminated timber deck systems. This deck system involved the use of glulam panels positioned such that the load was applied parallel to the wide face of the laminations. The glulam deck panels were tested in a laboratory under simulated AASHTO wheel loading criteria. Results of this testing indicated that an effective distribution of the wheel load across the panel width was achieved. Based on an analytical evaluation of the test data, glulam deck panels were modeled as an orthotropic plate with a continuous dimension in the direction parallel to the bridge span.

Gutkowski *et al* (1983) also reported that based on handling and manufacturing considerations, the optimum width for the individual deck panels is about 48 inches. In order to achieve continuity across the individual deck panels, a mechanical method for transferring both the shear and moment across the panel joints was developed. An effective method was steel dowels imbedded at the mid depth of the panels. Design equations and charts were developed for the design of both the deck panels, using orthotropic plate behavior, and the steel dowels using a beam on an elastic foundation model. It was found the doweled deck system required close manufacturing tolerances and was difficult to install in the field. The Weyerhaeuser Company developed a cast aluminum bracket to be used in lieu of the steel dowels to interconnect the transverse glulam deck panels with the girders. This deck bracket was bolted to the deck panel by the use of a bolt through the deck. A flange of the bracket then fits into a pre-routed groove in the side of the wooden girder. The groove is longer than the bracket flange to allow some adjustment. Sets of formed "teeth" on the bracket imbed themselves in both the deck and the wood girder. In the case of steel girders, steel clips are bolted to the deck and clamp onto the flange of the W-shape.

1.2.2 ASPHALT PAVEMENT WEARING SURFACES

Ritter (1992) describes an asphalt pavement wearing surface as a layer of bituminous concrete that is spread and compacted on the bridge deck to produce a smooth, well-consolidated surface. A wearing surface must interact with other bridge components for overall structural performance. The wearing surface is intended to wear away over a period of time and therefore its performance and integrity cannot be ensured for the life of the structure. The portion of the bridge that directly contacts passing vehicles is the wearing surface so it must provide good skid resistance to enhance user safety. One of the primary functions of the wearing surface is to protect the deck from wear and exposure to the elements. The most common asphalt wearing surface used on timber bridge decks is hot-mix asphalt.

The Asphalt Institute (1983) describes hot-mix asphalt as a combination of well-graded, high quality aggregate that is uniformly mixed and coated with asphalt cement. Hot-mix is manufactured at a central batching plant where aggregate and asphalt cement

are heated to 250 to 325 °F before mixing. While the paving mixture is still hot, it is trucked to the construction site where it is placed and compacted. Asphalt mixtures are produced from a wide range of mix designs involving aggregate combinations and type and quantity of asphalt. For most highway applications, a large aggregate base layer of hot-mix asphalt is topped with a smaller aggregate top layer of hot-mix asphalt and is sometimes used with a geotextile fabric.

Ritter (1992) describes geotextile fabrics as synthetic engineering fabrics that were originally developed to provide additional stability and load distribution in numerous geotechnical and hydraulic applications. When placed between the bridge deck and asphalt pavement, geotextile fabrics can improve the bond between the asphalt and the deck surface, provide increased moisture resistance of the surface, and reduce pavement cracking at glulam panel joints. Geotextile fabrics for bridge paving are available in two types; plain and asphalt impregnated (bituminized fabric sheets). Bituminized fabric sheets have a layer of rubberized asphalt bonded to one side and are available in widths up to 36 inches. The asphalt impregnated sheets are most commonly used on timber decks where the heat from the asphalt causes the rubberized asphalt layer to bond to the deck which provides improved adhesion and a good barrier to moisture.

1.2.3 FINITE ELEMENT MODELING OF TIMBER BRIDGE DECKS

Wipf et al. (1990) developed a finite element model to study the behavior of a glued laminated, longitudinal deck highway bridge. Experimental tests of a full scale laboratory test bridge were performed to validate the model. The bridge was a 26 ft span and used six 27 ft long, 48 in wide, 10-3/4 in thick glued laminated panels manufactured from Douglas Fir lumber. A general purpose finite element program, SAP IV (Bathe et al. 1973), was used to model the bridge. The glued laminated panels were modeled as thin plate/shell elements. Stiffener beams were modeled using three dimensional beam elements. For the experimental program, deflection measurements were taken at 6 in. from the center line of the bridge. Results showed a slightly larger displacement of the panels based on the analytical model prediction when compared to the experimental displacement. The authors concluded that the analytical model accurately predicted the behavior of the bridge and that the experimental results support the conservatism of the analytical model.

Davalos *et al* (1993) used a finite element program for general anisotropic shell type structures to determine effective width factors for stress laminated bridges. The finite element model was used for the analysis of single and double lane, simply supported timber bridge decks. The decks were modeled with 9-node degenerated isoparametric elements that included shear deformation. An AASHTO HS-20 truck loading was used in the study and the wheel loads were modeled as concentrated loads placed to produce the maximum moment. A convergence study of the mesh size indicated sufficiently accurate results were obtained using shell elements of 20 in by 22 in

for most of their analyses. The maximum deflection of the deck was used to obtain the effective widths for the stress laminated timber bridge decks. Effective width was computed by equating the maximum deflection in the bridge deck with the maximum deflection of a beam subjected to equivalent loading. The authors determined effective width factor of 0.6 for single lane and 0.7 for double lanes.

1.3 SCOPE AND PURPOSE FOR RESEARCH

As previously mentioned, the purpose for this study was to investigate the structural behavior of asphalt/wood/membrane deck systems. Deflection of full scale models of deck panels on a simulated girder bridge was measured. The specimens were analyzed using both classical and finite element models and the experimental and analytical results were compared. A method of calculating interpanel deck deflection is proposed.
The deflection criteria was applied to various configurations of asphalt/wood/membrane composites and an optimal arrangement was determined.

The details and results of the analytical investigation are presented in Chapter II. Chapter III outlines the experiemntal procedures and presents the experimental results. Comparisons and discussion of the experimental and analytical investigation results are provided in Chapter IV. Chapter V gives details of the proposed deck deflection design calculations.

CHAPTER II

ANALYTICAL INVESTIGATION OF GLULAM DECK PANELS

2.1 GENERAL

The analytical investigation of the behavior of asphalt/wood deck systems consists primarily of an interpanel deflection analysis. Deflection analysis involves modeling the deck as: 1) a simply supported beam; 2) a continuous beam. Both a classical and a finite element analysis of the deck were performed. Deflection of the beam is used to estimate a possible deck deflection of an actual bridge. The estimated differential deflection of adjacent glulam deck panels in a glulam girder bridge is used in the experimental investigation of the performance of various asphalt/membrane/glulam combinations. The theoretical equations derived in this chapter are used to estimate an effective modulus of elasticity from the experimental results and are presented in Chapter IV.

2.2 DEFLECTION ANALYSIS DETAILS

2.2.1 MEMBER GEOMETRY AND ASSUMPTIONS

The deflection analysis uses two cases to estimate the deflection of the glulam deck panel. A simply supported, pinned-roller configuration and a three span continuous, pinned support configuration are considered. Panels are modeled as beams and not as plates. This is a realistic assumption due to the large in-plane stiffness and geometry of the glulam deck panel. The simply supported beam is modeled as a Bernoulli-Euler beam which does not consider shear deflection since the ratio of span to depth are 28 and 21. Not considering shear deflection for an E/G ratio of 16 would result in an error of less than five percent for the simply supported beam. The continuous beam is modeled as a Mindlin beam since the span to depth ratio are 9 and 7. The Mindlin beam model assumes that although plane sections through the beam still remain straight and undeformed, they are not necessarily normal to the centroidal axis and this allows consideration for shear deflection. The loading is on the narrow face of the individual lamina as shown in Figure 2.1. The American Institute of Timber Construction (AITC, 1993) lists the modulus of elasticity in the y-y direction for southern yellow pine glulam as 1,500,000 psi. The supports are assumed to be rigid and there is no axial forces acting on the panel and hence, no axial displacements. The weight of the panel is ignored due to the relative magnitude of the loading and any geometric non-linearity or material non-linearity is assumed to be insignificant since the deflections are small compared to the size and configuration of the test panels.

2.2.3 Classical Method

The geometry for the simple beam is shown in Figure 2.2. The calculations are in terms of an applied load, *P*. The equation for shear in the beam, in terms of *x*, is shown in Equation 2.1.

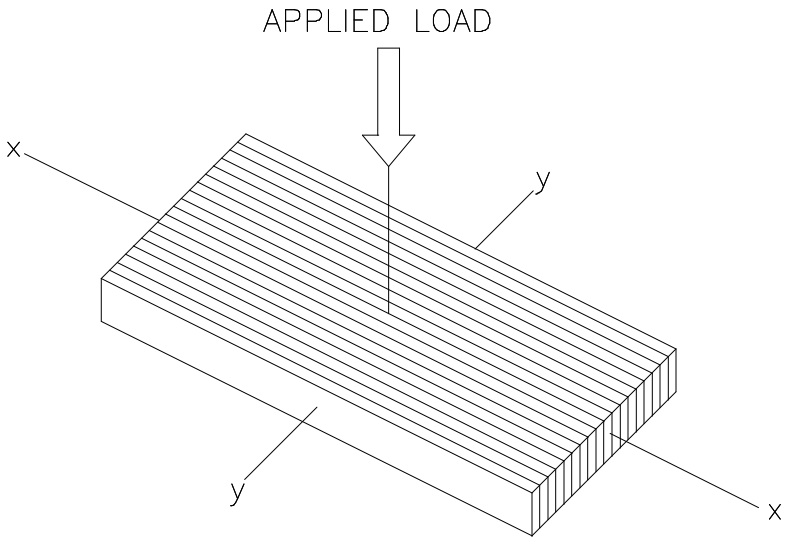

Figure 2.1 Panel Loading Configuration

$$V(x) = \frac{P}{2} - P\left\langle x - \frac{L}{2}\right\rangle^{0} \qquad \textbf{(2.1)}$$

where $\left\langle x - \frac{L}{2}\right\rangle^{0} = 1$ when $x \geq \frac{L}{2}$ and $= 0$ when $x < \frac{L}{2}$

The equation for moment in the beam in terms of *x* is

$$M(x) = \int V(x) = \frac{1}{2}Px - P\left\langle x - \frac{L}{2}\right\rangle^{1} \qquad \textbf{(2.2)}$$

where $\left\langle x - \frac{L}{2}\right\rangle^{1} = \left(x - \frac{L}{2}\right)$ when $x \geq \frac{L}{2}$ and $= 0$ when $x < \frac{L}{2}$

The governing differential equation for the elastic curve of a prismatic beam is

$$\frac{d^2 y_b}{dx^2} = \frac{M(x)}{EI} \qquad \text{which can be rewritten as} \quad M(x) = EI\frac{d^2 y_b}{dx^2} \tag{2.3}$$

Substituting Equation 2.2 into Equation 2.3, results in

$$EI\frac{d^2 y_b}{dx^2} = \frac{1}{2}Px - P\left\langle x - \frac{L}{2}\right\rangle^1 \tag{2.4}$$

Integrating Equation 2.4, results in the expression for the slope of the deflected shape (Equation 2.5) and the expression for deflection (Equation 2.6).

$$q = \frac{dy_b}{dx} = \frac{1}{EI}\left(\frac{1}{4}Px^2 - \frac{1}{2}P\left\langle x - \frac{L}{2}\right\rangle^2 + C_1\right) \tag{2.5}$$

$$y_b = \frac{1}{EI}\left(\frac{1}{12}Px^3 - \frac{1}{6}P\left\langle x - \frac{L}{2}\right\rangle^3 + C_1 x + C_2\right) \tag{2.6}$$

Boundary conditions are used to determine the constants C_1 and C_2:
At $x = 0, y_b = 0$, Substituting into Equation 2.6 gives:

$$0 = 0 - \frac{1}{6}P\left\langle 0 - \frac{L}{2}\right\rangle^3 + 0 + C_2 \quad \text{which yields } C_2 = 0$$

At $x = L$, $y_b = 0$ and substituting into Equation 2.6 gives:

$$0 = \frac{PL^3}{12} - \frac{P}{6}\left\langle L - \frac{l}{2}\right\rangle^3 + 0 + C_1 L$$

$$C_1 L = -\frac{PL^3}{12} + \frac{PL^3}{48} \quad \text{which yields} \quad C_1 = -\frac{PL^2}{16}$$

Substituting the constants into equation 2.6 and rearranging, results in the final expression for deflection,

$$y_b = \frac{1}{EI}\left[\frac{Px^3}{12} - \frac{P}{6}\left\langle x - \frac{L}{2}\right\rangle^3 - \frac{PL^2}{16}x\right] \tag{2.7}$$

The modulus of elasticity, $E_{y,}$ for southern yellow pine 24F-V3 glulam is 1,500,000 psi according to the American Institute of Timber Construction AITC 117-93

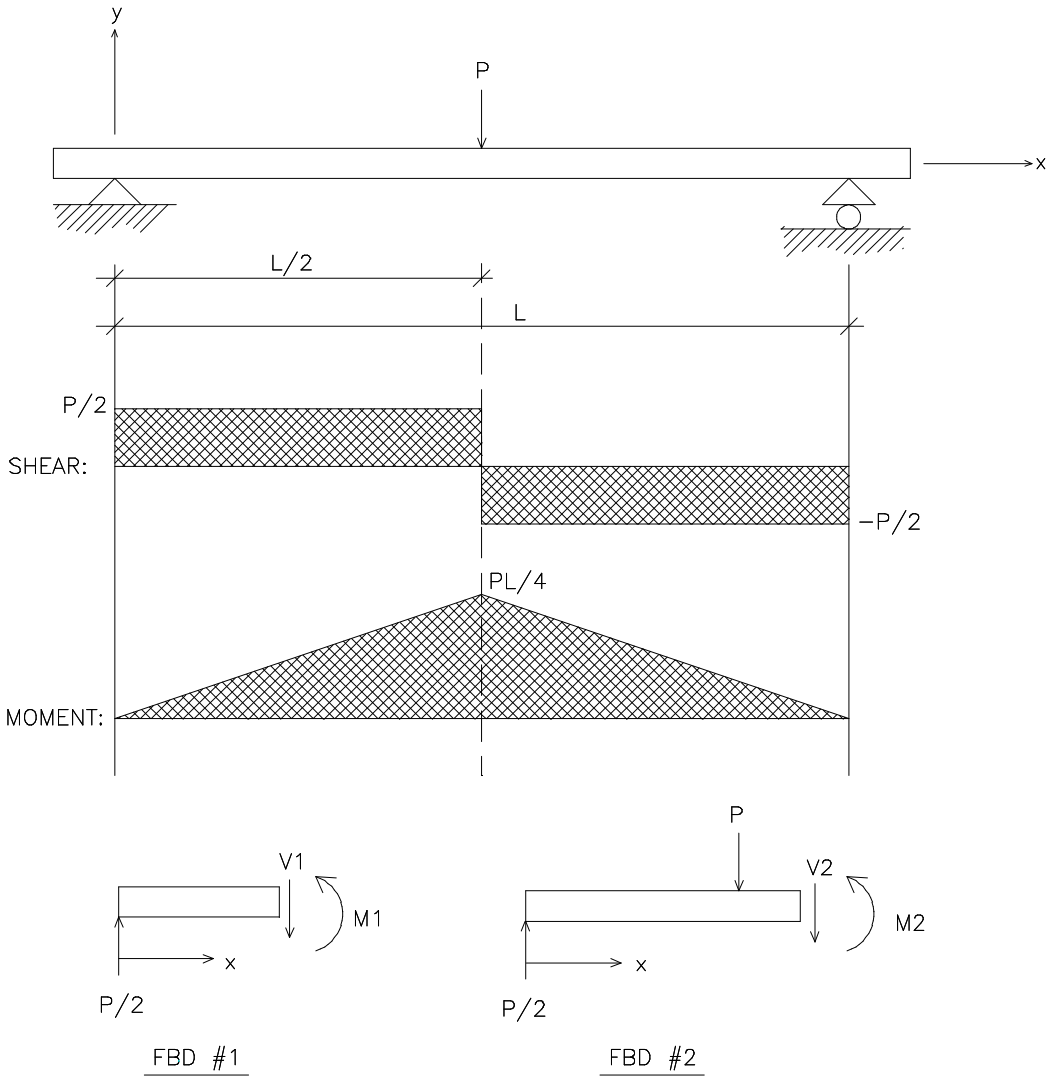

Figure 2.2 Simple Beam Analysis Configuration

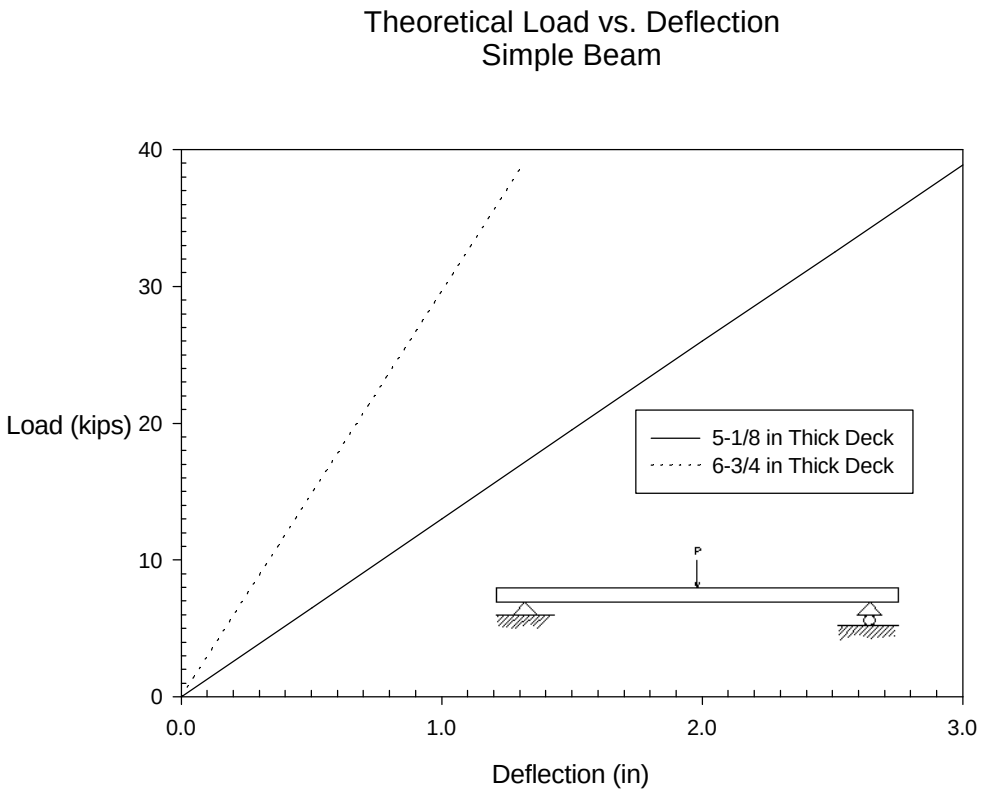

Figure 2.3 Simple Beam - Load vs. Deflection Plot

design guide. The calculated moment of inertia for the 5-1/8 in. thick by 48 in. wide deck panel is 538 in^4 and 1,230 in^4 for the 6-3/4 in. thick by 48 in. wide deck panel. The resulting load versus centerline deflection relationships for the two deck panels are shown in Figure 2.3.

Geometry for the continuous beam problem is shown in Figure 2.4. The calculations are in terms of two applied loads, *P*, applied at the center of the two outside spans and at the center of the panel width. The symmetrical loading of the continuous beam was considered in the development of the beam equations, and reaction forces were calculated with the aid of a plane frame analysis program.

The equation for shear force in the beam in terms of x, measured horizontally from the left support, is derived from FBD #5 on Figure 2.4 and is

$$V(x) = 0.425P - P\left\langle x - \frac{L}{2}\right\rangle^0 + 0.575P\langle x - L\rangle^0 + 0.575P\langle x - 2L\rangle^0 - P\left\langle x - \frac{5L}{2}\right\rangle \qquad \textbf{(2.8)}$$

where $\left\langle x - \frac{L}{2}\right\rangle^0 = 1$ when $x \geq \frac{L}{2}$, and $= 0$ when $x < \frac{L}{2}$;

$\langle x - L\rangle^0 = 1$ when $x \geq L$, and $= 0$ when $x < L$;

$\langle x - 2L\rangle^0 = 1$ when $x \geq 2L$, and $= 0$ when $x < 2L$; and

$\left\langle x - \frac{5L}{2}\right\rangle^0 = 1$ when $x \geq \frac{5L}{2}$, and $= 0$ when $x < \frac{5L}{2}$.

The equation for the moment in the continuous beam in terms of x is

$$M(x) = 0.425Px - P\left\langle x - \frac{L}{2}\right\rangle^1 + 0.575P\langle x - L\rangle^1 + 0.575P\langle x - 2L\rangle^1 - P\left\langle x - \frac{5L}{2}\right\rangle^1 \qquad \textbf{(2.9)}$$

where $\left\langle x-\frac{L}{2}\right\rangle^1 = \left(x-\frac{L}{2}\right)$ when $x \geq \frac{L}{2}$, and $=0$ when $x<\frac{L}{2}$;

$\langle x-L\rangle^1 = (x-L)$ when $x \geq L$, and $=0$ when $x<L$;

$\langle x-2L\rangle^1 = (x-2L)$ when $x \geq 2L$, and $=0$ when $x<2L$;

and $\left\langle x-\frac{5L}{2}\right\rangle^1 = \left(x-\frac{5L}{2}\right)$ when $x \geq \frac{5L}{2}$, and $=0$ when $x<\frac{5L}{2}$.

Recalling that the governing differential equation for the elastic curve of a prismatic beam is

$$M(x) = EI\frac{d^2y_b}{dx^2} \tag{2.3}$$

Substituting Equation 2.9 into Equation 2.3 results in

$$EI\frac{d^2y_b}{dx^2} = 0.425Px - P\left\langle x-\frac{L}{2}\right\rangle^1 + 0.575P\langle x-L\rangle^1 + 0.575P\langle x-2L\rangle^1 - P\left\langle x-\frac{5L}{2}\right\rangle^1 \tag{2.10}$$

Integrating Equation 2.10 results in the expression for the slope of the deflected shape (Equation 2.11) and the expression for flexural deflection (Equation 2.12).

$$q = \frac{dy_b}{dx} = \frac{1}{EI}\left(0.213Px^2 - \frac{1}{2}P\left\langle x-\frac{L}{2}\right\rangle^2 + 0.288P\langle x-L\rangle^2 + 0.288P\langle x-2L\rangle^2 - \frac{1}{2}P\left\langle x-\frac{5L}{2}\right\rangle^2 + C_1\right) \tag{2.11}$$

$$y_b = \frac{1}{EI}\left(0.071Px^3 - \frac{1}{6}P\left\langle x-\frac{L}{2}\right\rangle^3 + 0.096P\langle x-L\rangle^3 + 0.096P\langle x-2L\rangle^3 - \frac{1}{6}P\left\langle x-\frac{5L}{2}\right\rangle^3 + C_1x + C_2\right) \tag{2.12}$$

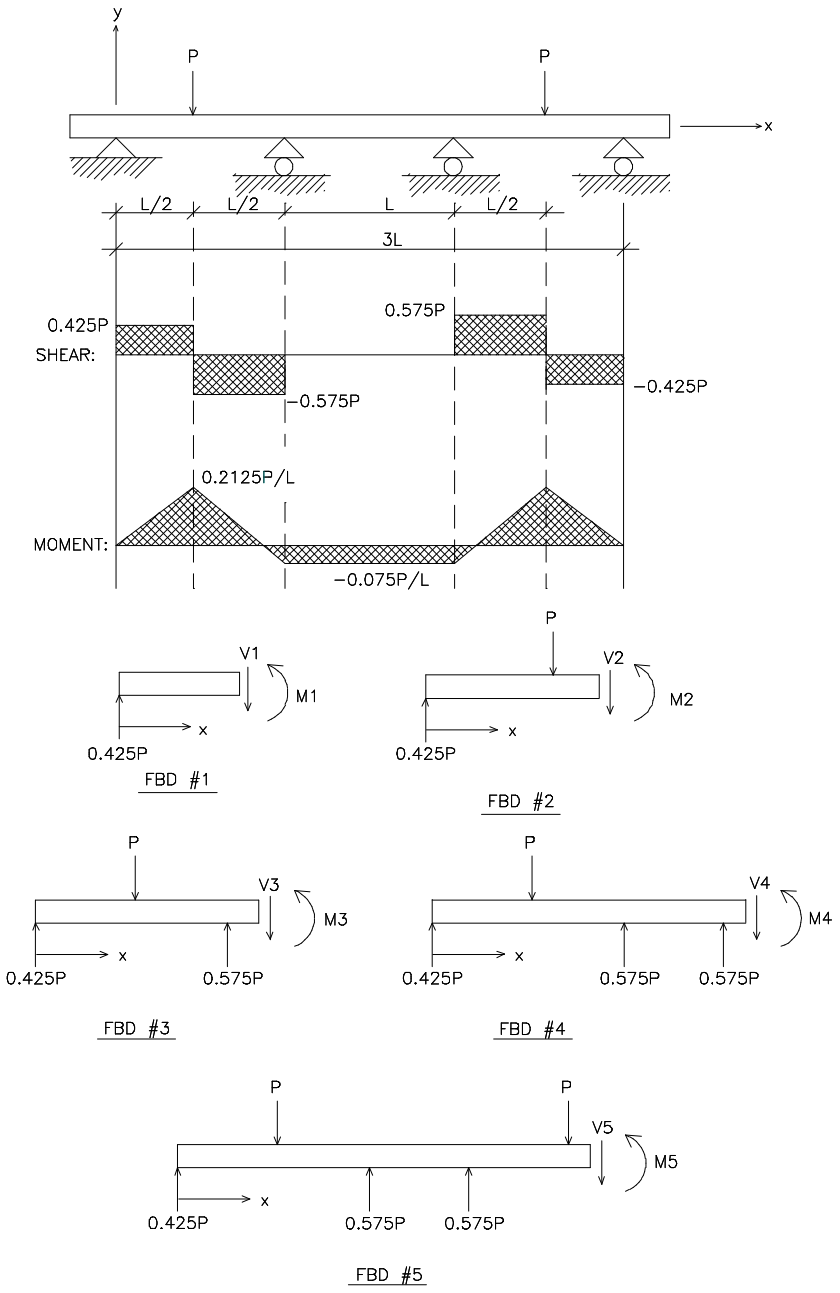

Figure 2.4 Continuous Beam Analysis Configuration

The boundary conditions are used to determine the constants C_1 and C_2.
At $x = 0$, $y_b = 0$ and substituting into Equation 2.12 gives:

$$0 = 0 - \frac{1}{6}P\left\langle 0 - \frac{L}{2}\right\rangle^3 + 0.096P\langle 0 - L\rangle^3 + 0.096P\langle 0 - 2L\rangle^3 - \frac{1}{6}P\left\langle 0 - \frac{L}{2}\right\rangle^3 + 0 + C_2$$

which yields $C_2 = 0$

At $x = L$, $y_b = 0$ and substituting into Equation 2.12 gives:

$$0 = 0.071PL^3 - \frac{1}{6}P\left\langle L - \frac{L}{2}\right\rangle^3 + 0.096P\langle L - L\rangle^3 + 0.096P\langle L - 2L\rangle^3 - \frac{1}{6}P\left\langle L - \frac{5L}{2}\right\rangle^3 + C_1L + 0$$

Solving for C_1L ,

$$C_1L = -0.071PL^3 + \frac{PL^3}{48} - 0$$

which yields $$C_1 = -0.05PL^2$$

Substituting the constants into Equation 2.12 and rearranging, results in the final expression for deflection due to flexure of the beam

$$y_b = \frac{1}{EI}\left[0.071Px^3 - \frac{1}{6}P\left\langle x - \frac{L}{2}\right\rangle^3 + 0.096P\langle x - L\rangle^3 + 0.096P\langle x - 2L\rangle^3 - \frac{1}{6}P\left\langle x - \frac{5L}{2}\right\rangle^3 - 0.05PL^2x\right] \quad \textbf{(2.13)}$$

Due to the fact that the span-to-depth ratio of the deck panel is 9.36 for the 5-1/8 in. thick deck and 7.11 for the 6-3/4 in. thick deck the beam is modeled as a Mindlin beam and shear deformation is considered. The expression for shear deflection (Timeshenko,1955) is

$$y_v = \frac{1}{2}\frac{E}{G}\left(\frac{d}{L}\right)^2 y_b \qquad \textbf{(2.14)}$$

where E is the modulus of elasticity, G is the modulus of rigidity, d is the depth of the beam, L is the length of the side of the deck panel normal to the direction along which y_v is measured (equal to span length, L, defined earlier), and y_b is the deflection due to flexure calculated from Equation 2.13.

As indicated in the 1991 National Design Specification for Wood Construction **(**AFPA, 1993**)** , the modulus of rigidity for southern yellow pine is approximately 1/16 the modulus of elasticity. Therefore, the modulus of rigidity, G, is approximately 100,000 psi. Using a span length, L, of 48 in., the load versus deflection relationship (point load applied at the center of an outside span) for the continuous beam was developed and is shown in Figure 2.5. Both flexure and shear deflections were considered and the deflection was calculated for the point directly under the applied point load. The plot for the classical method is linear since the deflection varies linearly with the applied load and this is demonstrated in Figure 2.5. Shear deflection contributed eight percent for the 5-1/8 in. thick deck and thirteen percent for the 6-3/4 in. deck with respect to the total deflection. A comparison of the deflection caused by flexure and shear is presented in Table 2.1.

2.2.3 FINITE ELEMENT METHOD

A finite element model of the experimental deck panels used in the deflection test was developed using shell elements in the commercial finite element program Sap90 (Wilson and Habibullah, 1995). The shell elements used were four node, isoparametric formulation including rotational stiffness components both in-plane and in the direction normal to the plane of the element. These elements include shear deflection in the the analysis of the total deflection. An eight point numerical integration scheme was used for the elements, and forces and moments were evaluated at the integration points and extrapolated to the joints of the element.

The 144 in. by 48 in. deck panels were modeled with 144 shell elements each 4 in. by 12 in. and either 5-1/8 in. or 6-3/4 in. thick. The mesh of the finite element model is shown in Figure 2.6. Loads were applied at the nodes across the width of the deck panel to emulate the line load applied in the experiment. The left restraint was modeled as a pin while all other restraints were modeled as rollers. The finite element model was analyzed at six different loadings for each of the deck thicknesses and configurations for a total of twenty-four runs. The same assumptions used in the classical models were used in the finite models, i.e. modulus of elasticity is 1,500,000 psi and only small deformations occur. Typical finite element input files are provided in Appendix B.

2.3 DEFLECTION ANALYSIS RESULTS

Results of the finite element model closely tracked that of the classical model and are shown in Tables 2.1-A, 2.1-B, 2.2-A and 2.2-B. The difference between the classical and the finite element model are less than two percent except for the 6-3/4 in continuous beam which differed by approximately six percent. Figure 2.8 clearly shows the finite model is more stiff than the classical model. Figure 2.7 shows the values to be approximately equal with the differences being attributed to round-off errors or the possible exclusion of shear deflection in the simple beam classical model. The load for an AASHTO HS 20-44 is approximately 16 kips per wheel so by looking at the plot on Figure 2-5 one can estimate the deflection to be approximately 0.04 in for the 5-1/8 in thick deck panel. Since there are many different spacings of girders in actual bridges, 0.05 in differential deflection was chosen as a typical value and used in the experimental portion of the study. Theoretical values and finite element values are shown in Figures 2.7 and 2.8 which again demonstrates the linearity and the similarity of the two methods.

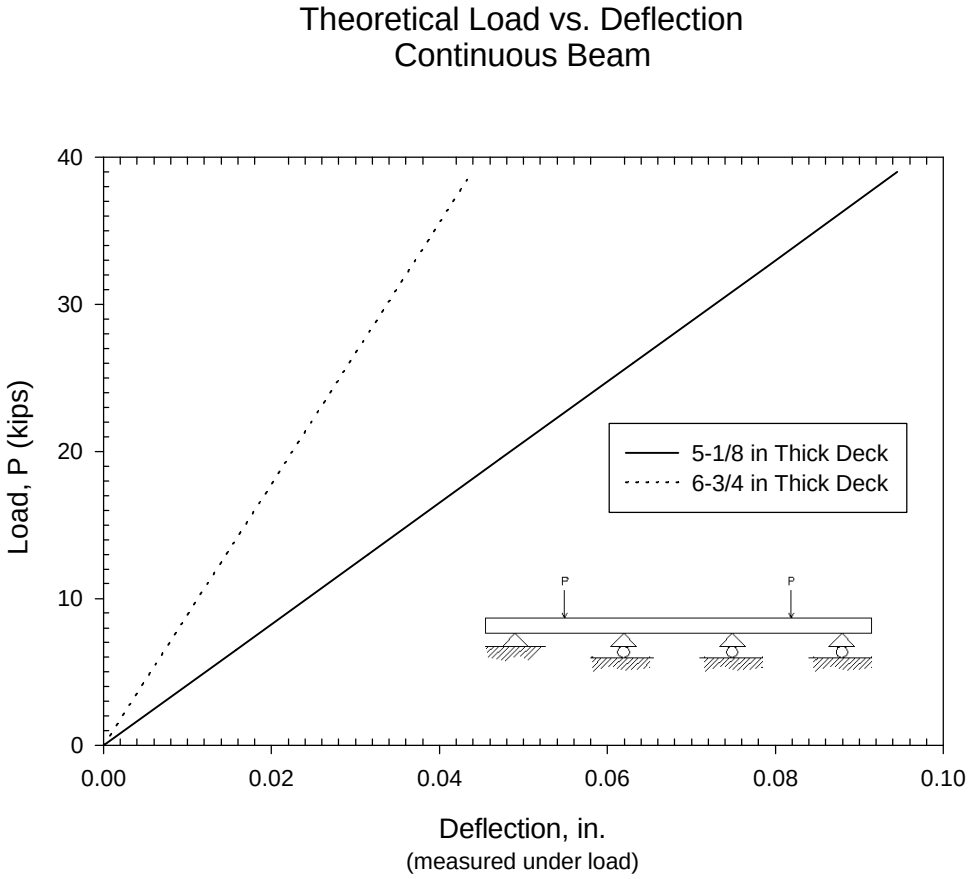

Figure 2.5 Continuous Beam - Load vs. Deflection Plot

Table 2.1 Flexural and Shear Deformation Comparison

5-1/8" Thick - Continuous Beam				
Load (kips)	**Flexural Δ (inches)**	**Shear Δ (inches)**	**Total Δ (inches)**	**% Shear Δ**
6.5	0.0144	0.0013	0.0158	8.36
13.0	0.0289	0.0026	0.0315	8.36
19.5	0.0433	0.0039	0.0473	8.36
26.0	0.0578	0.0053	0.0630	8.36
32.5	0.0722	0.0066	0.0788	8.36
39.0	0.0866	0.0079	0.0945	8.36
6-3/4" Thick - Continuous Beam				
Load (kips)	**Flexural Δ (inches)**	**Shear Δ (inches)**	**Total Δ (inches)**	**% Shear Δ**
6.5	0.0063	0.0010	0.0073	13.66
13.0	0.0126	0.0020	0.0146	13.66
19.5	0.0190	0.0030	0.0219	13.66
26.0	0.0253	0.0040	0.0293	13.66
32.5	0.0316	0.0050	0.0366	13.66
39.0	0.0379	0.0060	0.0439	13.66

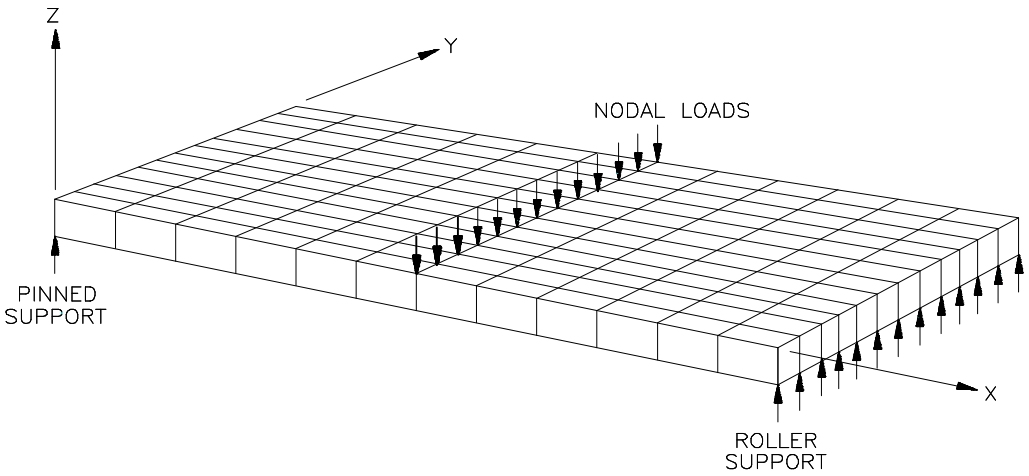

a) Finite Element Mesh for Simple Beam

NOTE: Shell element thickness either 5-1/8 in. or 6-3/4 in. Nodal loads were applied at 13 nodes for simple beam

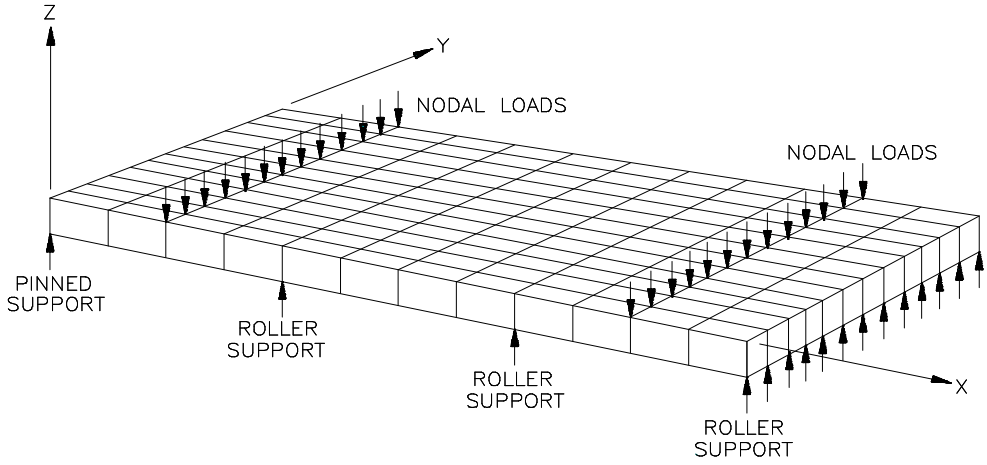

b) Finite Element Mesh for Continuous Beam

NOTE: Shell element thickness either 5-1/8 in. or 6-3/4 in. Nodal loads were applied at 26 nodes for continuous beam

Figure 2.6 Finite Element Model Configurations

Table 2.2-A Simple Beam Classical and Finite Element Model Results

5-1/8 in. SIMPLE BEAM			
LOAD (kips)	CLASSICAL ANALYSIS DEFLECTION (inches)	FE ANALYSIS DEFLECTION (inches)	DIFFERENCE (%)
6.5	0.5010	0.5090	1.6
13.0	1.000	1.020	2.0
19.5	1.500	1.530	2.0
26	2.000	2.030	1.5
32.5	2.510	2.540	1.2
39	3.010	3.050	1.3

Table 2.2-B Continuous Beam Classical and Finite Element Model Results

5-1/8 in. CONTINUOUS BEAM			
LOAD (kips)	CLASSICAL ANALYSIS DEFLECTION (inches)	FE ANALYSIS DEFLECTION (inches)	DIFFERENCE (%)
6.5	0.0158	0.0160	1.3
13.0	0.0315	0.0310	1.6
19.5	0.0473	0.0470	0.6
26	0.0630	0.0620	1.6
32.5	0.0788	0.0780	1.0
39	0.0945	0.0930	1.6

Table 2.3-A Simple Beam Classical and Finite Element Model Results

6-3/4 in. SIMPLE BEAM			
LOAD (kips)	CLASSICAL ANALYSIS DEFLECTION (inches)	FE ANALYSIS DEFLECTION (inches)	DIFFERENCE (%)
6.5	0.2190	0.2230	1.8
13.0	0.4380	0.4450	1.6
19.5	0.6570	0.6680	1.7
26	0.8770	0.8910	1.6
32.5	1.0960	1.1130	1.6
39	1.3150	1.3360	1.6

Table 2.3-B Continuous Beam Classical and Finite Element Model Results

6-3/4 in. CONTINUOUS BEAM			
LOAD (kips)	CLASSICAL ANALYSIS DEFLECTION (inches)	FE ANALYSIS DEFLECTION (inches)	DIFFERENCE (%)
6.5	0.0070	0.0068	2.9
13.0	0.0140	0.0136	2.9
19.5	0.0210	0.0205	2.4
26	0.0280	0.0273	2.6
32.5	0.0350	0.0340	2.9
39	0.0420	0.0408	2.9

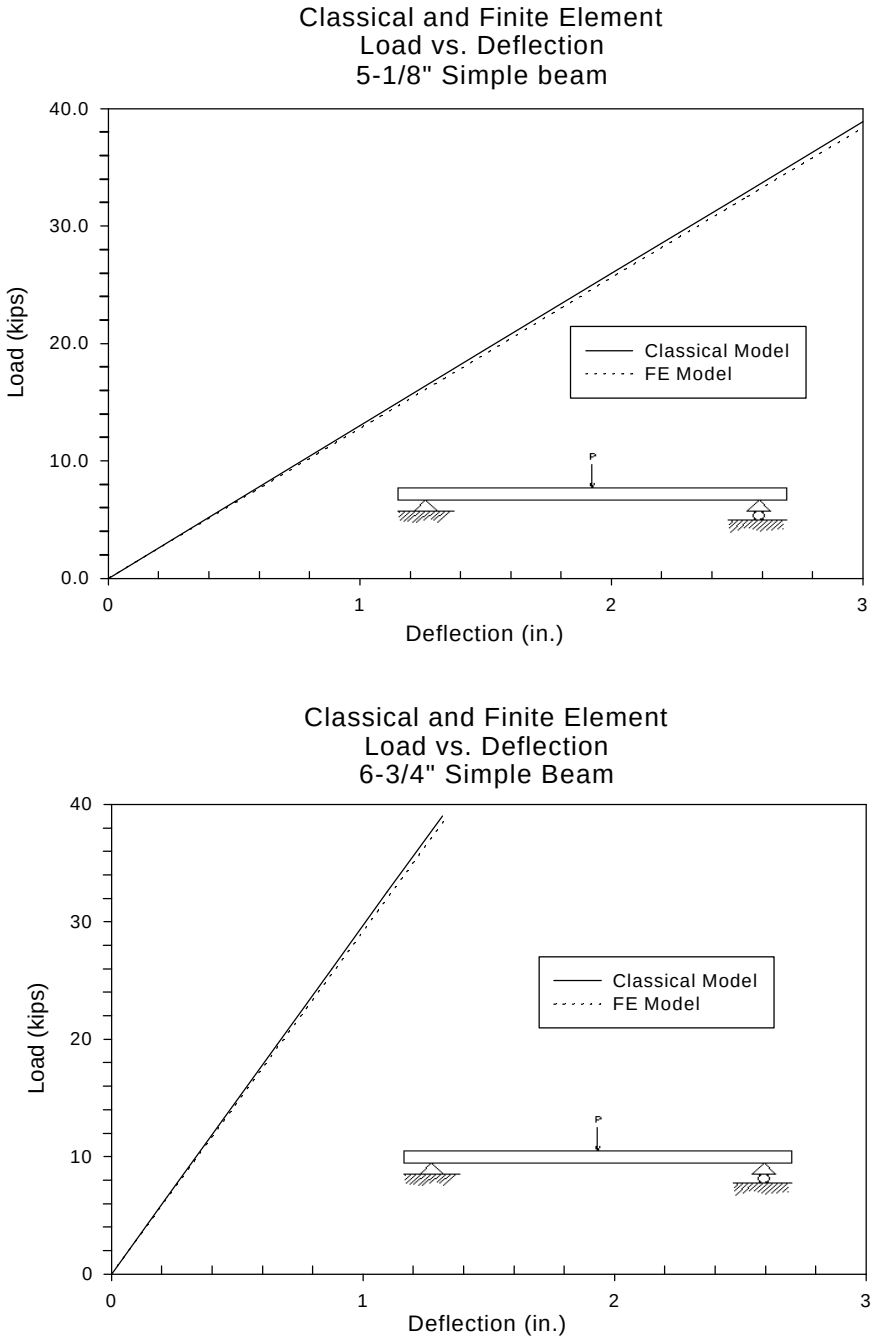

Figure 2.7 Simple Beam - Classical and Finite Element Comparison

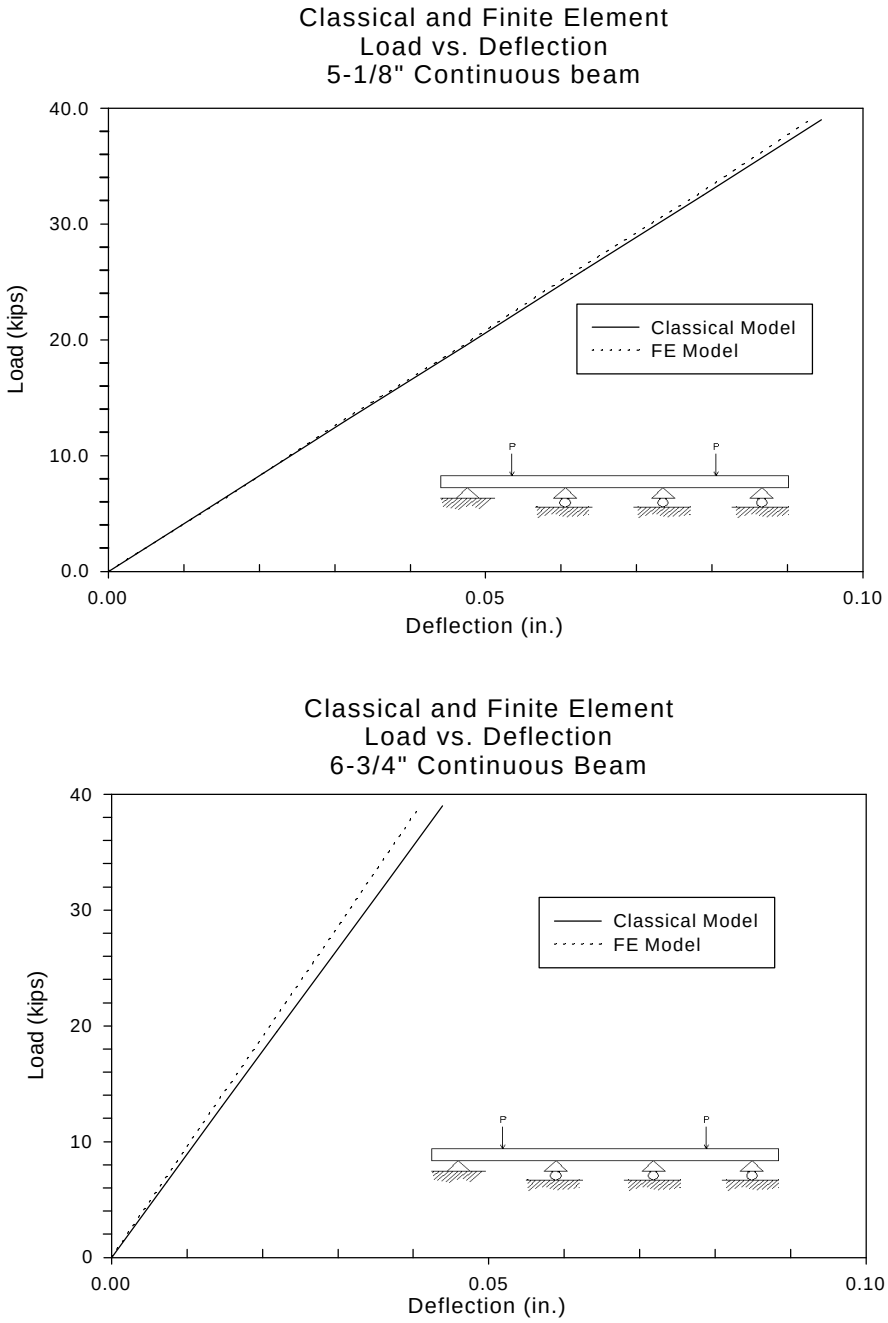

Figure 2.8 Continuous Beam - Classical and Finite Element Comparison

CHAPTER III

EXPERIMENTAL INVESTIGATION OF GLULAM DECK PANELS AND WEARING SURFACE OVERLAYS

3.1 SCOPE OF TESTING

Two distinctly different but related tests were conducted in this study. The first test determined an effective modulus of elasticity for glued laminated bridge deck panels subjected to flexure. The MOE was used to calculate the deflection of a deck panel supported as a continuous beam. This deflection is termed "interpanel deck deflection" and is the deflection of one deck panel with respect to an adjacent deck panel. The second test consisted of asphalt/wood/membrane composites subjected to repeated interpanel deck deflections. Determining the behavior of various deck overlay configurations, with respect to crack propagation, was the objective of this test.

3.1.1 Interpanel Deck Deflections

Four deflection tests on four separate samples of glued laminated deck panels, for a total of sixteen tests, were conducted at the Virginia Tech Structures and Materials Research Laboratory in Blacksburg, Virginia. The tests were performed to determine reasonable interpanel deck deflections to be used in the asphalt cracking tests.

Each test specimen consisted of a glulam deck panel supported by glulam girders in both single span and three span configurations as shown in Figure 3.1. Test setups were constructed to emulate a typical timber girder bridge configuration. Specimens were subjected to an applied vertical force so that the maximum deflection of the panel could be determined. The specimens were instrumented (i.e. load and deflection were measured), loaded and an effective modulus of elasticity was calculated.

3.1.2 Asphalt Crack Promulgation

A total of twenty-two tests of asphalt/wood/membrane configurations were conducted at the Virginia Tech Structures and Materials Research Laboratory in Blacksburg, Virginia. The tests were conducted to determine the best configuration for paving timber bridge decks.

Each test specimen consisted of two 2 ft by 5 ft glulam panels placed adjacent to each other and then covered with various asphalt/membrane configurations. Specimens were placed in a single span beam setup and one panel was loaded which created a differential deflection between the two panels at their interface. The load was cyclic and

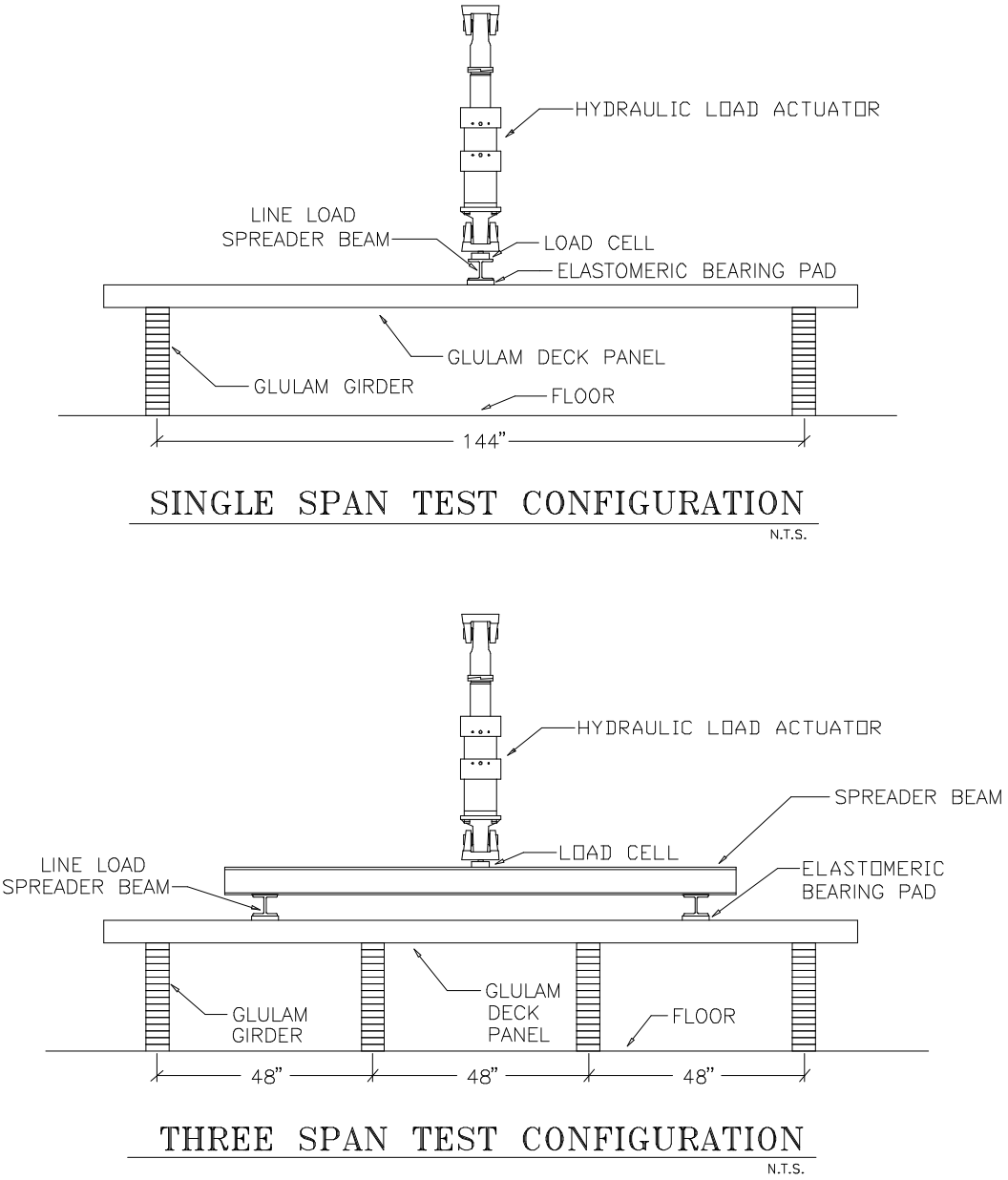

Figure 3.1 Typical Deflection Test Configurations

of suficient magnitude to obtain the cyclic and of sufficient magnitude to obtain the deflection determined by the initial deflection test results. The test configuration is shown in Figure 2.2. Three different membranes and two different types of hot-mix asphalt were used in the various panel configurations. Specimens were visually monitored for any cracking in the asphalt along the interface line of the two glulam deck panels. The test configuration attempted to emulate the expected interpanel deflection of a typical glulam deck panel and determine the optimal configuration for the asphalt-membrane layers.

3.2 DEFLECTION TEST DETAILS

3.2.1 Deflection Test Specimens

Deflection test specimens were fabricated by Unit Structures Specialty Products Group, Inc. in Morrisville, North Carolina. All glulam deck panels were constructed of Southern Yellow Pine in accordance with AITC Standards. The panels had a 24F-V3 lay-up and were AITC industrial appearance grade. The test panels were not pressure treated with preservatives or fire retardant chemicals but in practice preservative chemicals are essential to provide longevity. Deck panels were fabricated in two configurations; two specimens were 5-1/8 in by 48 in by 14 ft and two specimens were 6-3/4 in by 48 in by 14 ft. Four glulam girders were laminated in the same manner as the deck panels and were 5-1/8 in by 24-3/4 in by 12 ft long. Aluminum deck mounting clips, manufactured by Laminated Concepts in Elmira, New York, were used for some tests to attach the deck panels to the girders while the other tests used simple supports.

3.2.2 Deflection Test Setup

Two different loading configurations, each with two different reaction boundary conditions, were used in the deflection tests. The test matrix is shown in Table 3.1. The three span loading configuration was used to emulate an actual bridge and the single span loading configuration was used the increase the panel length to depth ratio. The three span configuration was loaded equally on each of the outside spans with line load spreader beams distributing the load across the width of the deck panel. The length for each of the three spans was 48 in. The single span configuration was loaded in the center of the 144 in span length also using line load spreader beams. As shown in Figure 3.3, a knife-edge support was used in one boundary condition in order to simulate a pinned connection and facilitate comparison to theoretical models and aluminum deck clips were used in the other boundary condition in order to simulate typical construction practices.

3.2.3 Deflection Test Instrumentation

Test data was obtained through the use of displacement transducers (LVTD's and rotary potentiometers) and load cells. All instrumentation was connected to a PC-based data acquisition system which was used to record the data during the test. The applied load and various displacements were recorded during the tests. The location of the instrumentation is shown on Figure 3.4.

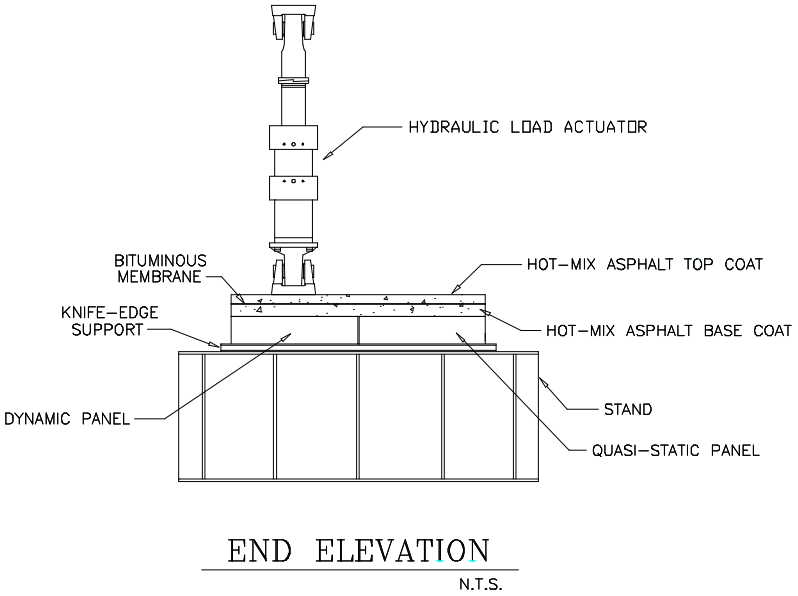

Figure 3.2 Typical Asphalt Cracking Test Configuration

Table 3.1 Deflection Test Matrix

Test Designation	Load Configuration	Boundary Conditions	Panel Dimensions(in)
Panel-1	1 Span	Knife-Edge	5-1/8 x 48 x 168
Panel-2	3 Span	Knife-Edge	5-1/8 x 48 x 168
Panel-3	3 Span	Deck-Clips	5-1/8 x 48 x 168
Panel-4	1 Span	Deck-Clips	5-1/8 x 48 x 168
Panel-5	1 Span	Knife-Edge	5-1/8 x 48 x 168
Panel-6	3 Span	Knife-Edge	5-1/8 x 48 x 168
Panel-7	3 Span	Deck-Clips	5-1/8 x 48 x 168
Panel-8	1 Span	Deck-Clips	5-1/8 x 48 x 168
Panel-9	1 Span	Knife-Edge	6-3/4 x 48 x 168
Panel-10	3 Span	Knife-Edge	6-3/4 x 48 x 168
Panel-11	3 Span	Deck-Clips	6-3/4 x 48 x 168
Panel-12	1 Span	Deck-Clips	6-3/4 x 48 x 168
Panel-13	1 Span	Knife-Edge	6-3/4 x 48 x 168
Panel-14	3 Span	Knife-Edge	6-3/4 x 48 x 168
Panel-15	3 Span	Deck-Clips	6-3/4 x 48 x 168
Panel-16	1 Span	Deck-Clips	6-3/4 x 48 x 168

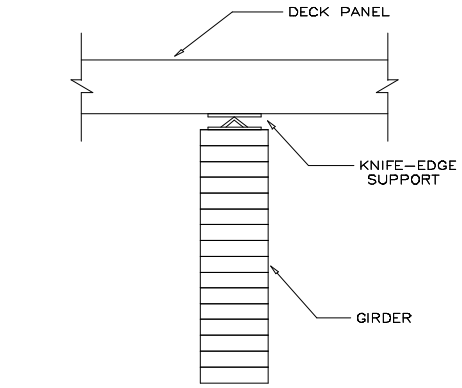

KNIFE–EDGE SUPPORT

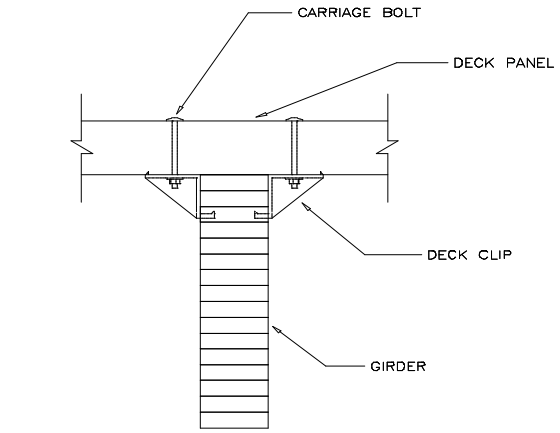

DECK CLIP SUPPORT

Figure 3.3 Deflection Test Boundary Conditions

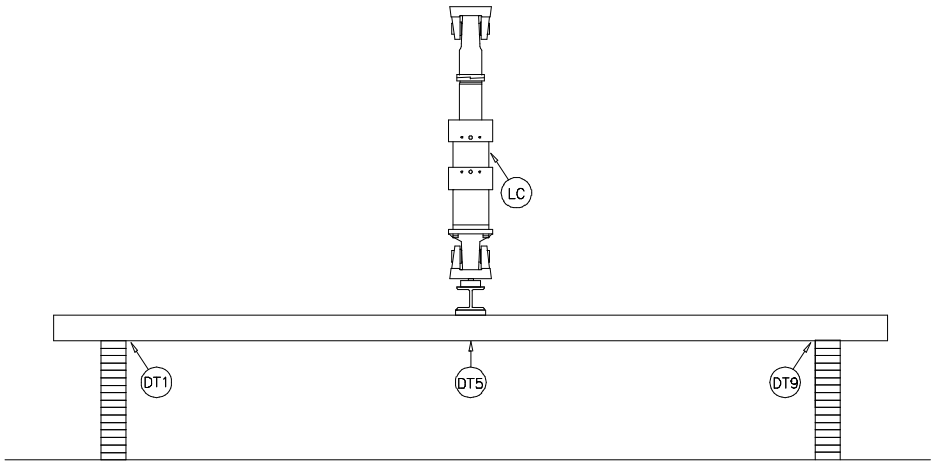

SINGLE SPAN TEST CONFIGURATION

N.T.S.

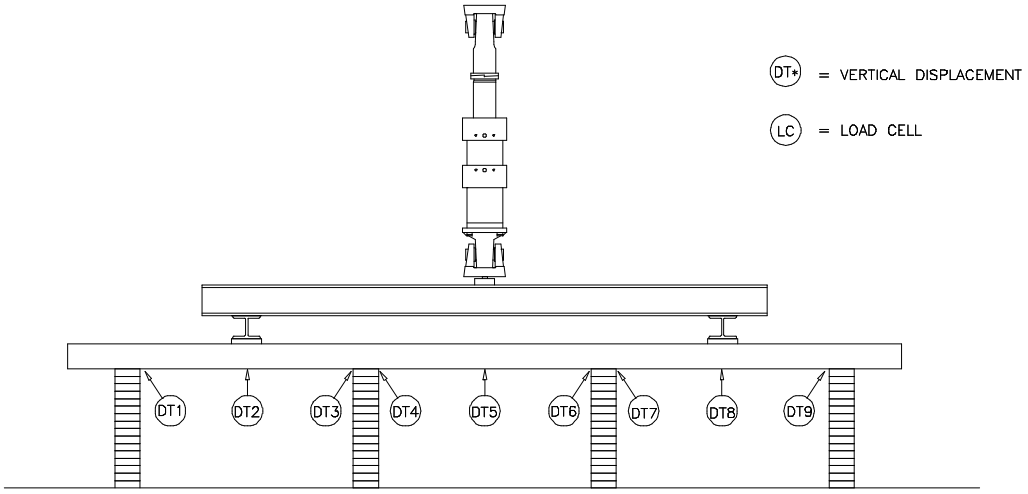

THREE SPAN TEST CONFIGURATION

N.T.S.

Figure 3.4 Deflection Instrumentation Location

3.2.4 Deflection Test Procedure

Once the test configuration and instrumentation were properly positioned, the test was started. After taking initial readings the load was applied in approximately 5 kip increments up to about 20 kips. All instrumentation was checked to ensure readings were near computed theoretical values and the specimen was unloaded. The specimen was incrementally loaded again and then unloaded. At each load increment, instrumentation readings were recorded and a plots were made of load versus absolute deflection of the deck panels. The objective of this test was to obtain an effective modulus of elasticity for the glulam deck panels so the specimens were loaded only below the proportional limit.

3.3 DEFLECTION TEST RESULTS

Comparative results are summarized in Table 3.2. The panels were all loaded in flexure and acted like beams instead of plates. The possible plate action was examined by loading across the width of the deck panel at various locations. The resulting deflections were the same across the width therefore plate behavior was not exhibited. The single span configuration had a span to depth ratio of 21.33 so it demonstrated Bernoulli/Euler beam behavior. The three span setup had a span to depth ratio of 7.11 so shear deflection should be considered in the analysis. Complete test results including plots, specimen dimensions, and test observations can be found in Appendix A. The average deflection for the single span, 5-1/8 in thick specimens was 1.434 in when subjected to a load of 30 kips. This translates to an average effective modulus of elasticity of 2,400,000 psi.

The average deflection for the single span, 6-3/4 in thick specimens was 0.841 in when subjected to a load of 30 kips. This translates to an average effective modulus of 1,800,000 psi. The equations used to calculate the effective moduli of elasticity are provided in Chapter III. A load versus deflection plot for the average experimental results for the simple beam is shown in Figure 3.5. The average deflection for the three span, 5-1/8 in thick specimens was 0.046 in when subjected to a load of 30 kips. This translates to an average effective modulus of elasticity of 2,300,000 psi. The average deflection for the three span, 6-3/4 in thick specimens was 0.040 in when subjected to a load of 30 kips. This translates to an average effective modulus of 1,300,000 psi. A load versus deflection plot for the average experimental results for the simple beam is shown in Figure 3.6.

3.4 CRACKING TEST DETAILS

3.4.1 Cracking Test Specimens

The cracking test glulam panels were fabricated by Laminated Timbers, Inc. in London, Kentucky. The glulam panels were constructed of Southern Yellow Pine with a

waterproof adhesive in accordance with AITC Standards. The panels had a 24F-V3 lay-up and were AITC industrial appearance grade. The panels were not pressure treated with preservatives or fire retardant chemicals and were 5 in. by 24 in. by 60 in. with no camber.

Three different bituminized fabric sheets were used in the asphalt cracking tests: M400A Waterproof Membrane fabricated by the Protecto Wrap Company, Denver, Colorado; Petrotac Self-Adhesive Nonwoven Fabric manufactured by Phillips Fiber Corporation, Greenville, South Carolina; and Bituthene 5000 supplied by W.R. Grace Company, Cambridge, Massachusetts.

Two hot-mix asphalt mixtures were used in the asphalt cracking test; Virginia Department of Transportation's BM-2 base course and Virginia Department of Transportation's SM-2A surface mix. The asphalt content of each of the mixes was determined according to ASTM D 2172. Gradation analysis was performed according to ASTM C 117 and C136. The asphalt contents and gradations for each of the mixes are reported in Table 3.3.

3.4.2 Cracking Test Setup

Twelve different asphalt/wood/membrane configurations were used in the cracking tests. The test matrix is shown in Table 3.4. Two glulam deck panels were placed side by side to form a 48 in by 60 in surface and temporarily attached to each other with 4 by 4 in timbers and lag bolts. The panels were then paved with various configurations of hot-mix asphalt and geotextile membranes. The entire sample was then placed on stands in the testing frame and the 4 by 4 in timbers were removed. A 6 in strip of whitewash was painted on the asphalt top directly above and along the panel interface in order to improve visibility of any cracking. The desire was to emulate the deflection of a continuous beam as would be experienced in an actual bridge, therefore the span was shortened from 48 in to 44 in. This shorter span is the length between the points of zero curvature on the continuous beam analysis. The load footprint was 12 in. by 20 in. which is a similar aspect ratio as that provided by truck tires. The loading block was constructed of wood and had rounded edges where in contact with the asphalt as shown in Figure 3.7.

3.4.3 Cracking Test Instrumentation

Displacement transducers were placed at the adjacent edges of each glulam panel in the center of the span. A hydraulic actuator was used to provide the interpanel cyclic deflection. All instrumentation was connected to a PC based data acquisition system which was used to monitor the interpanel deflection and count the number of load cycles. The location of the instrumentation is shown on Figure 3.7.

Table 3.2 Comparative Deflection Test Summary

Test Designation	Applied Load (kips)	TD2 Deflection (in)	TD5 Deflection (in)	TD8 Deflection (in)
Panel-1	30.061	N/A	1.436	N/A
Panel-2	30.073	0.055	N/A	0.050
Panel-3	29.998	0.047	N/A	0.041
Panel-4	30.053	N/A	1.311	N/A
Panel-5	30.052	N/A	1.554	N/A
Panel-6	30.039	0.044	N/A	0.043
Panel-7	30.070	0.042	N/A	0.048
Panel-8	30.031	N/A	1.435	N/A
Panel-9	30.084	N/A	0.843	N/A
Panel-10	29.920	0.053	N/A	0.030
Panel-11	30.047	0.047	N/A	0.023
Panel-12	30.019	N/A	0.799	N/A
Panel-13	30.030	N/A	0.896	N/A
Panel-14	30.027	0.056	N/A	0.048
Panel-15	30.098	0.050	N/A	0.024
Panel-16	30.034	N/A	0.827	N/A

3.4.4 Cracking Test Procedure

Once the test specimen was in place, the stability attachments removed and the instrumentation placement was completed, the test was started. Load was applied at the center of one deck panel and the load was adjusted until the predetermined estimated differential deflection between the deck panels was obtained. The hydraulic actuator was controlled by a sinusoidal input source which allowed the deflection to vary from zero to the maximum deflection in one cycle. The counter was initialized and the load was applied at a frequency of about 3 Hz. The hydraulic actuator was programmed to stop after every 5,000 cycles to allow inspection for cracking. The test was then continued until the composite panel was fully cracked or 90,000 cycles was reached. 90,000 cycles is an estimate of the number of cycles a typical secondary bridge could experience due to truck traffic in two years.

3.5 Cracking Test Results

The cracking test results are difficult to quantify due to the fact that the asphalt tended to debond from the glulam deck panel and relieve the applied stress in that manner. The specimens that had the membrane placed directly between the asphalt overlay and the glulam deck panel showed cracking before 90,000 cycles almost universally. The membrane acted as an adhesive between the asphalt and the glulam and effectively transferred the applied strain due to the differential interpanel deflection and hence the cracking. The specimens that either did not contain a membrane or contained a membrane placed between two layers of asphalt performed the best, i.e., did not show any visual signs of cracking at the end of 90,000 cycles.

The results of the asphalt cracking test are tabulated in Table 3.5. Three of the tests were performed with a differential deflection of 0.15 in which would be the deflection of a 24 in wide, 5-1/8 in thick panel placed across girders spaced 48 in apart. The remaining tests were performed with a 0.05 in differential deflection modeling a 48 in wide, 5-1/8 in thick panel placed across girders spaced 48 in apart.

Although debondment of the asphalt is not a significant problem in actual structures, if a waterproofing membrane is desired, then the best configuration appears to be a membrane between a base layer of hot mix asphalt and a surface layer of hot mix asphalt. One should carefully examine the design applied loading to evaluate whether possible shoving of the asphalt (plastic flow or slipping of the bituminous wearing course when there is little bonding between layers) could occur. Further information addressing this issue can be found in Haramis (1997).

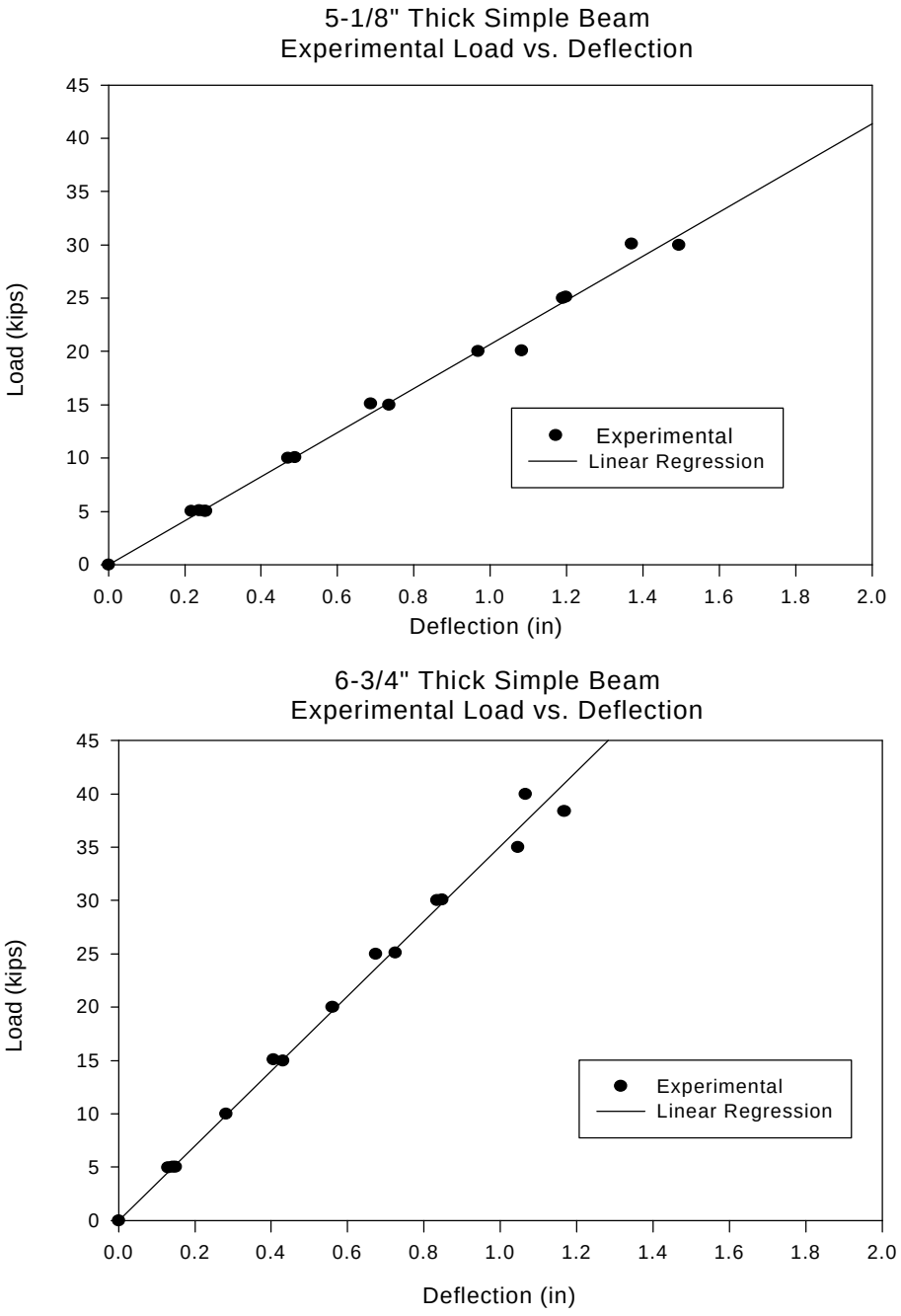

Figure 3.5 Experimental Load vs. Deflection - Simple Beam

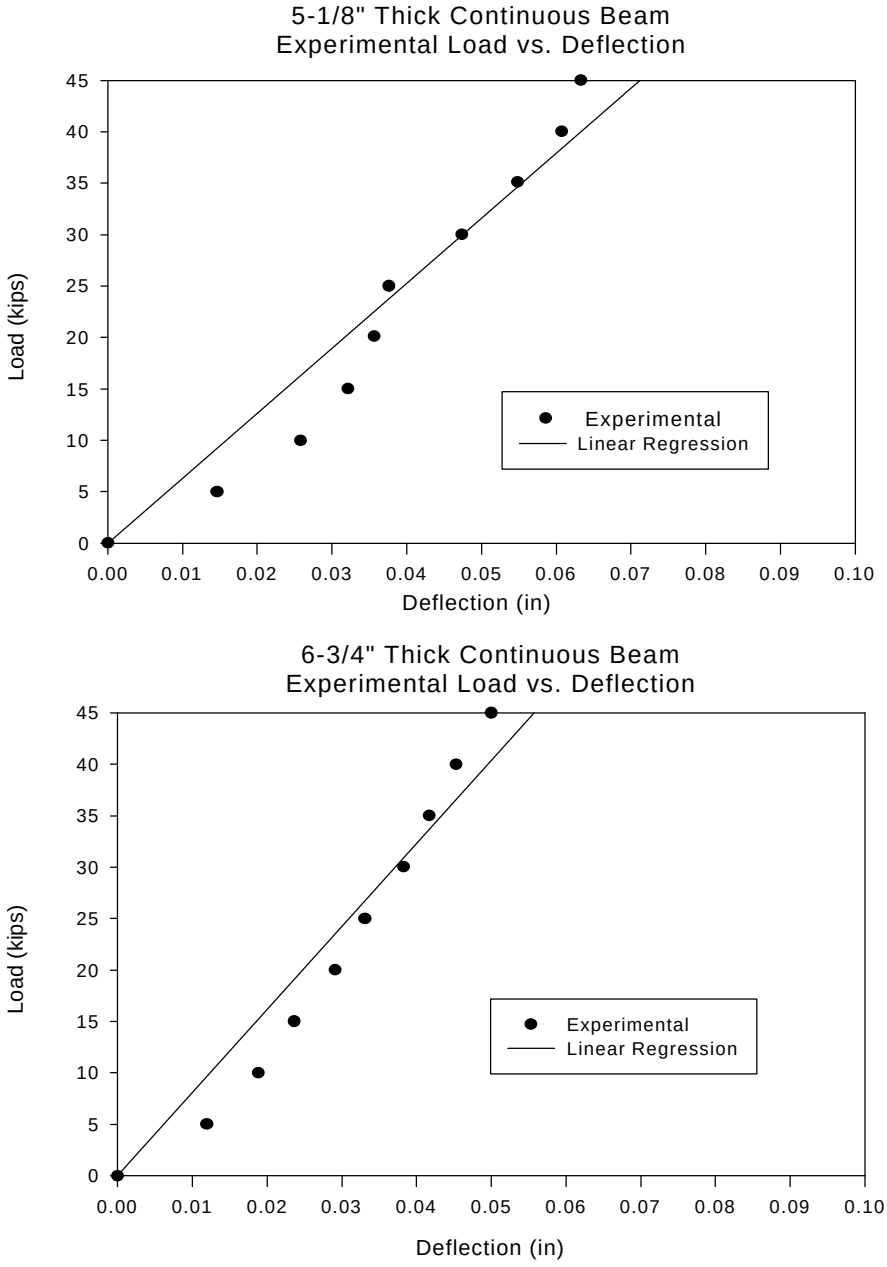

Figure 3.6 Experimental Load vs. Deflection - Continuous Beam

Table 3.3 Asphalt Content and Gradation of Test Mixtures

Sample	VDOT BM-2	VDOT SM-2AL
Sieve Size (mm)	Percent Passing	
25	100	100
19	93	100
12.5	72	100
9.5	62	92
4.75	48	65
2.36	29	41
1.18	18	27
0.60	13	19
0.30	10	15
0.15	8	13
0.075	7	11
Asphalt Content (%)	4.7	5.8

Table 3.4 Cracking Test Matrix

Configuration	Deflection (in)	Hot-Mix Asphalt	Membrane
Specimen 1	0.15	1-1/2” SM-2	None
Specimen 1	0.05	1-1/2” SM-2	None
Specimen 2a	0.15	1-1/2” SM-2	Bituthene
Specimen 2a	0.05	1-1/2” SM-2	Bituthene
Specimen 2a	0.05	1-1/2” SM-2	Bituthene
Specimen 2b	0.15	1-1/2” SM-2	Petrotac
Specimen 2b	0.05	1-1/2” SM-2	Petrotac
Specimen 2b	0.05	1-1/2” SM-2	Petrotac
Specimen 2c	0.05	1-1/2” SM-2	Protectowrap
Specimen 2c	0.05	1-1/2” SM-2	Protectowrap
Specimen 3	0.05	1-1/4” SM-2, 3” BM-2	None
Specimen 3	0.05	1-1/4” SM-2, 3” BM-2	None
Specimen 4a	0.05	1-1/4” SM-2, 3” BM-2	Bituthene
Specimen 4a	0.05	1-1/4” SM-2, 3” BM-2	Bituthene
Specimen 4b	0.05	1-1/4” SM-2, 3” BM-2	Petrotac
Specimen 4b	0.05	1-1/4” SM-2, 3” BM-2	Petrotac
Specimen 4c	0.05	1-1/4” SM-2, 3” BM-2	Protectowrap
Specimen 4c	0.05	1-1/4” SM-2, 3” BM-2	Protectowrap
Specimen 5	0.05	1” SM-2, 1-1/2” BM-2	None
Specimen 6a	0.05	1” SM-2, 1-1/2” BM-2	Bituthene
Specimen 6b	0.05	1” SM-2, 1-1/2” BM-2	Petrotac
Specimen 6c	0.05	1” SM-2, 1-1/2” BM-2	Protectowrap

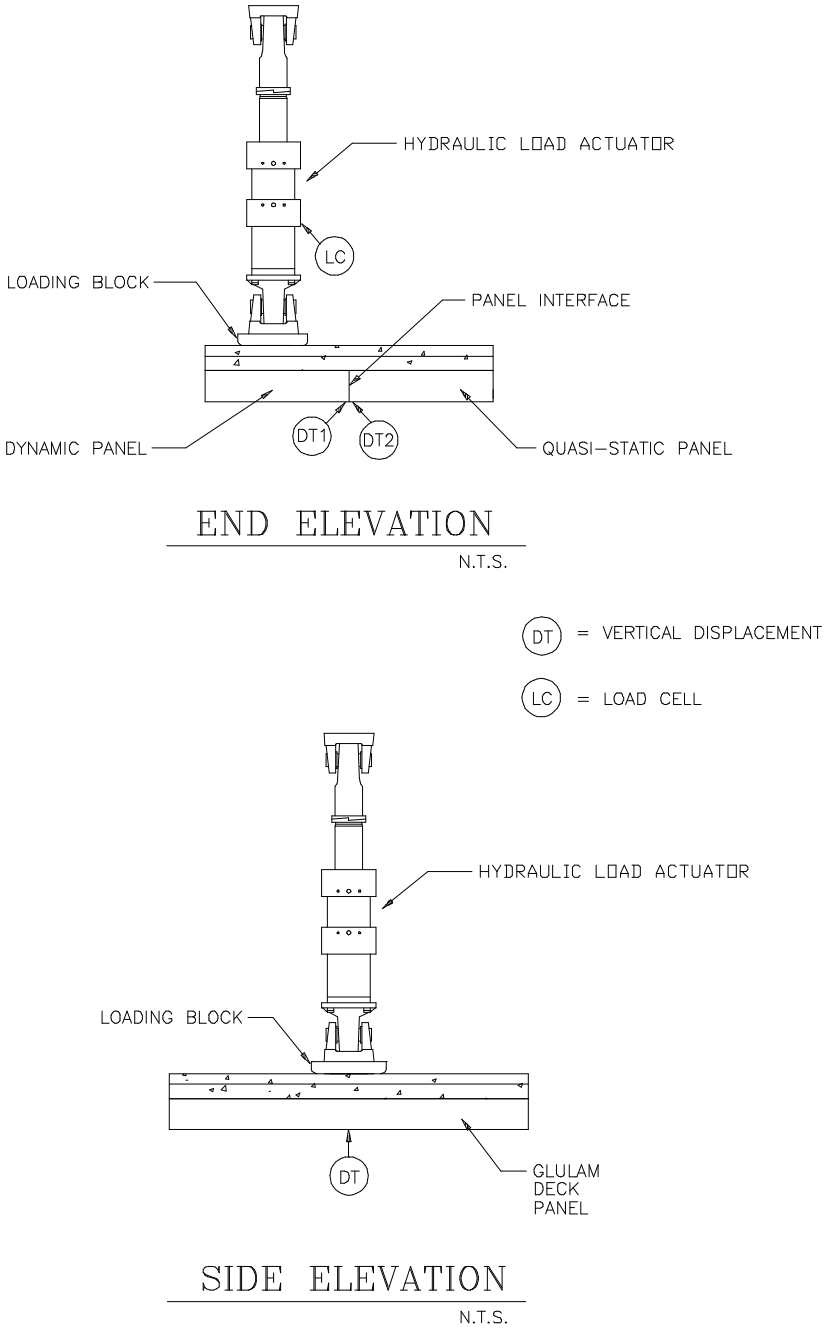

Figure 3.7 Cracking Test Instrumentation Location

Table 3.5 Cracking Test Summary

Configuration	Deflection (in)	Cycles	Results
Specimen 1	0.15	90,000	No Cracking
Specimen 1	0.05	90,000	No Cracking
Specimen 2a	0.15	10,000	Cracked
Specimen 2a	0.05	90,000	Crack Initiated
Specimen 2a	0.05	60,000	Cracked
Specimen 2b	0.15	1,000	Cracked
Specimen 2b	0.05	40,000	Cracked
Specimen 2b	0.05	36,000	Cracked
Specimen 2c	0.05	30,000	Cracked
Specimen 2c	0.05	32,000	Cracked
Specimen 3	0.05	90,000	No Cracking
Specimen 3	0.05	90,000	No Cracking
Specimen 4a	0.05	90,000	No Cracking
Specimen 4a	0.05	90,000	No Cracking
Specimen 4b	0.05	90,000	No Cracking
Specimen 4b	0.05	90,000	No Cracking
Specimen 4c	0.05	90,000	No Cracking
Specimen 4c	0.05	90,000	No Cracking
Specimen 5	0.05	90,000	No Cracking
Specimen 6a	0.05	90,000	No Cracking
Specimen 6b	0.05	90,000	No Cracking
Specimen 6c	0.05	90,000	No Cracking

CHAPTER IV

ANALYTICAL AND EXPERIMENTAL RESULTS

4.1 INTERPANEL DECK DEFLECTIONS

The results from the experimental investigations are found in Tables 3.1 and 3.2, Figures 3.5 and 3.6, and Appendix A. Figures 3.5 and 3.6 have been redrawn with 95% confidence interval lines in Figures 4.1 and 4.2. The plots in Figure 4.1 show that for the simple beams a few data points fall outside the confidence interval but most fall within. The plots in Figure 4.2 show that for the continuous beams significantly more data points fall outside the confidence interval. This can possibly be explained by the lower magnitude of deflection measured for the continuous beam compared to the simple beam (the stroke of the displacement transducers was two inches), greater influence of shear deflections on the continuous beam, or the increased possibility of instrumentation error due to settling of the test configuration during loading.

A linear regression was performed on each of the average results for each deck thickness and test configuration. The regression equations allow the experimental results to be more easily compared to the theoretical results. The regression equations are in the standard linear slope-intercept form, $y = mx + b$, where y is the load in kips and x is the deflection in inches. The y-intercept is forced to be equal to zero to emulate the circumstances in the actual experiment, in other words, the deflection is zero when the applied load is zero. These regression equations and comparative results for the experimental investigation are shown in Table 4.1.

The effective modulus of elasticity for the deck thickness and deflections given in Table 4.1 is calculated from the linear elastic equations developed in Section 3.2.3 and are tabulated in Table 4.2. The range of the effective modulus of elasticity is 1,400,000 to 2,400,000 psi which is quite a large difference. Calculated effective modulus of elasticity for each test is provided in Appendix A and is summarized in Table 4.3. The mean value for the M.O.E., determined by averaging the individual tests, is 1,950,000 psi and the standard deviation is 400,000 psi. If only the 5-1/8 in. thick decks are compared, the mean value for the M.O.E. is 2,300,000 psi with a standard deviation of 70,000 psi. If only the 6-3/4 in. thick decks are compared, the mean value for the M.O.E. is 1,600,000 psi with a standard deviation of 85,000 psi. There should not be this much difference between the two sizes of deck panels. The American Institute of Timber Construction (AITC, 1993) lists the modulus of elasticity of southern yellow pine as 1,500,000 psi.

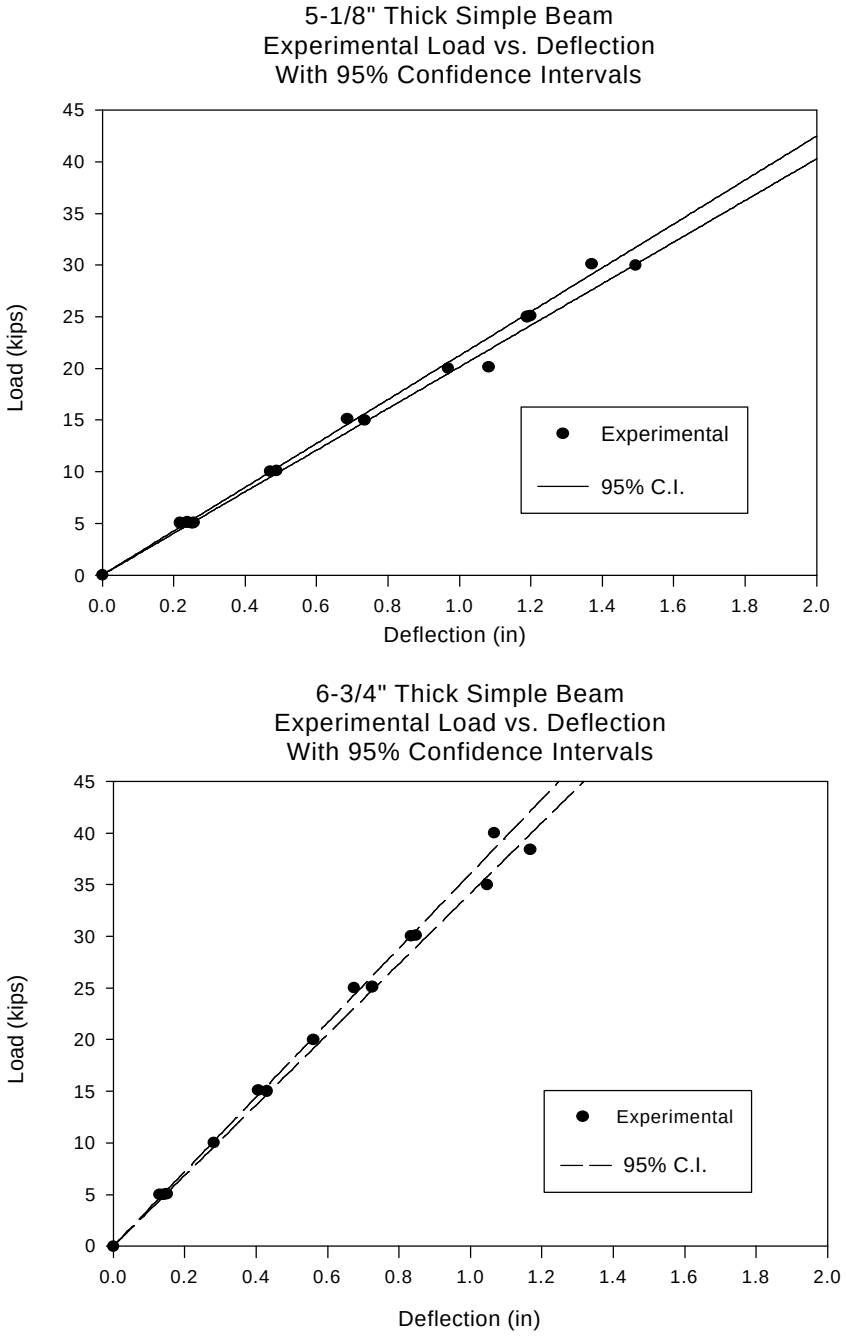

Figure 4.1 Experimental Load vs. Deflection With Confidence Intervals For Simple Beams

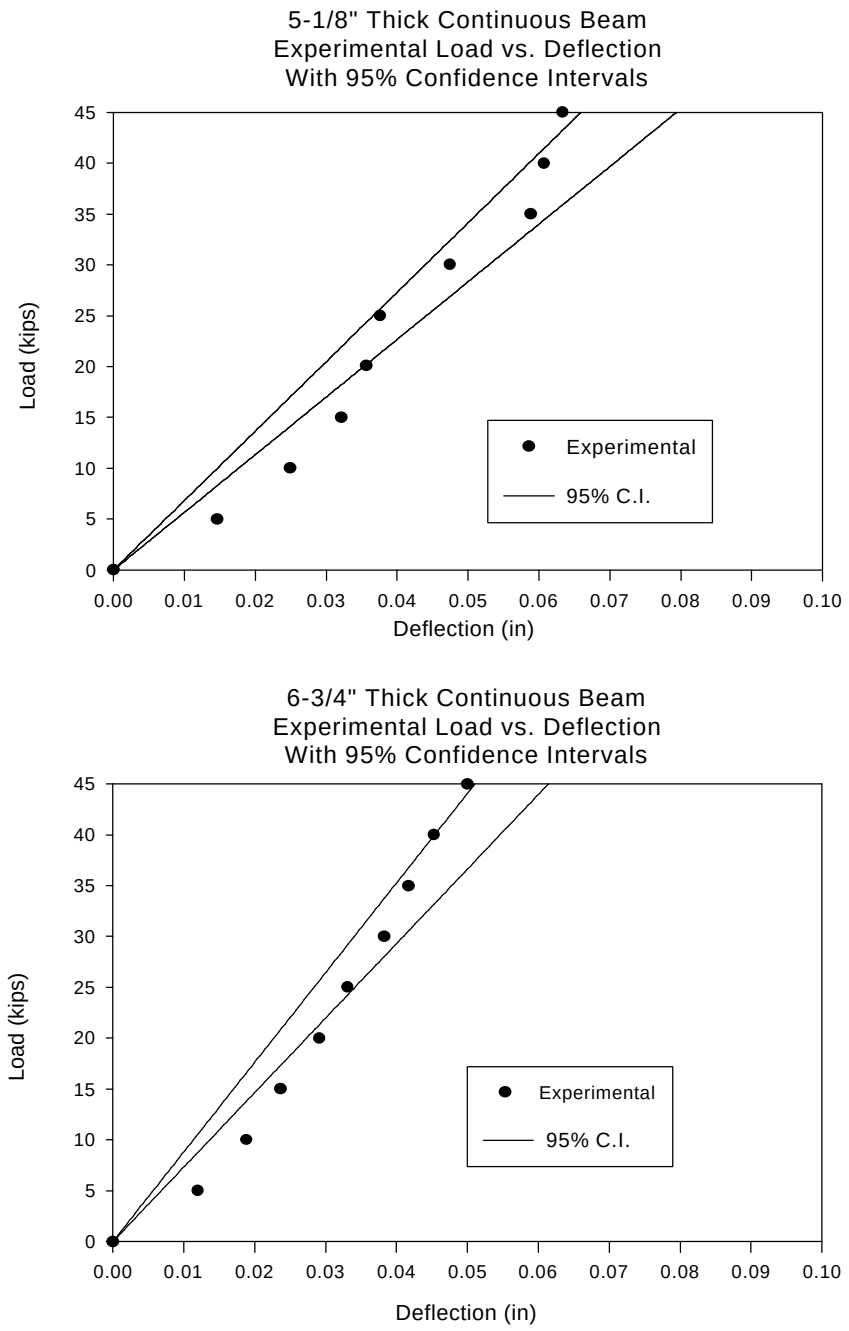

Figure 4.2 Experimental Load vs. Deflection With Confidence Intervals For Continuous Beams

Table 4.1 Comparative Experimental results

DECK THICKNESS	TEST CONFIGURATION	REGRESSION EQUATION	LOAD (kips)	DEFLECTION (inches)
5-1/8 in	Simple	y = 20.7 x	25	1.208
6-3/4 in	Simple	y = 35.1 x	25	0.712
5-1/8 in	Continuous	y = 608 x	25	0.041
6-3/4 in	Continuous	y = 798 x	25	0.031

Table 4.2 Average Modulus of Elasticity Results

DECK THICKNESS	TEST CONFIGURATION	LOAD (kips)	DEFLECTION (inches)	EFFECTIVE M.O.E. (psi)
5-1/8 in	SIMPLE	25	1.208	2,400,000
6-3/4 in	SIMPLE	25	0.712	1,800,000
5-1/8 in	CONTINUOUS	25	0.041	2,200,000
6-3/4 in	CONTINUOUS	25	0.031	1,400,000

Table 4.3 Modulus of Elasticity Results

TEST DESIGNATION	CONFIGURATION	THICKNESS	EFFECTIVE M.O.E.
PANEL 1	SIMPLE	5-1/8	2,400,000
PANEL 2	CONTINUOUS	5-1/8	2,000,000
PANEL 3	CONTINUOUS	5-1/8	2,100,000
PANEL 4	SIMPLE	5-1/8	2,600,000
PANEL 5	SIMPLE	5-1/8	2,200,000
PANEL 6	CONTINUOUS	5-1/8	2,300,000
PANEL 7	CONTINUOUS	5-1/8	2,400,000
PANEL 8	SIMPLE	5-1/8	2,400,000
PANEL 9	SIMPLE	6-3/4	1,800,000
PANEL 10	CONTINUOUS	6-3/4	1,400,000
PANEL 11	CONTINUOUS	6-3/4	1,500,000
PANEL 12	SIMPLE	6-3/4	1,900,000
PANEL 13	SIMPLE	6-3/4	1,700,000
PANEL 14	CONTINUOUS	6-3/4	1,200,000
PANEL 15	CONTINUOUS	6-3/4	1,500,000
PANEL 16	SIMPLE	6-3/4	1,800,000

The plots for the deflection tests in Appendix A show some interesting results. All of the plots for the simple beam configuration, whether 5-1/8 in. or 6-3/4 in. thick, are linear and are more stiff, i.e. have a greater modulus of elasticity, than specified. The plots for the continuous beam configuration are not nearly as linear. Most of the continuous beam plots, when the deflections of the two outside spans are averaged, tend to be linear. Test designations Panel 3, Panel 6, and Panel 10 show an increasing stiffness with increasing load during the initial loading portion of the graph and then a return to a more linear shape during the latter loading portion of the graph. Sometimes this indicates some type of cantenary action in the beam or deck where an axial load is increasing the stiffness of the beam. Cantenary action is unlikely with the test configuration and a more probable explanation is an initial settling and alignment of the test specimen during the early loading sequence. The data was conservatively modified by removing a data point with a smaller deflection and same loading as another data point.

The objective of the deflection tests is to predict the interpanel differential deflection when appropriate loads are applied. Considering the three span continuous test approximates the behavior of a bridge deck and estimating an AASHTO HS 20-44 truck load as two 16,000 lb. point loads, then a predicted interpanel differential deflection can be determined. Table 4.4 is compiled from the linear regression plot for the average of the two outside span deflections.

Table 4.4 Comparative Deflections for Experimental Continuous Configuration

TEST DESIGNATION	**LOAD (kips)**	**THICKNESS (in.)**	**EFFECTIVE M.O.E. (psi)**	**DEFLECTION (in.)**
PANEL 2	16	5-1/8	2,000,000	0.028
PANEL 3	16	5-1/8	2,100,000	0.027
PANEL 6	16	5-1/8	2,300,000	0.025
PANEL 7	16	5-1/8	2,400,000	0.023
PANEL 10	16	6-3/4	1,400,000	0.022
PANEL 11	16	6-3/4	1,500,000	0.018
PANEL 14	16	6-3/4	1,200,000	0.023
PANEL 15	16	6-3/4	1,500,000	0.018

4.2 ASPHALT/WOOD BEHAVIOR

The results from the experimental investigations are found in Table 3.5. Three specimens were subjected to 0.15 in. interpanel differential deflections and nineteen were subjected to 0.05 in. interpanel differential deflections. Specimen 1, consisting of 1-1/2 in. of surface mix asphalt placed directly on the deck surface without a membrane, was subjected to both 0.15 in. and 0.05 in. deflections for 90,000 cycles without showing any visible indication of cracking. Specimen 2a, consisting of a Bituthene membrane placed between 1-1/2 in. of surface mix asphalt and the deck surface, cracked after being subjected to 0.15 in. for 10,000 cycles and cracked after being subjected to 0.05 in. deflections for 60,000 cycles. Specimen 2b, consisting of a Petrotac membrane placed between 1-1/2 in. of surface mix asphalt and the deck surface, cracked after being subjected to 0.15 in. for 1,000 cycles and cracked after being subjected to 0.05 in. deflections for 40,000 cycles. Specimen 2c, consisting of a Protectowrap membrane placed between 1-1/2 in. of surface mix asphalt and the deck surface, cracked after being subjected to 0.05 in. deflections for 30,000 cycles. The remaining specimens did not crack after being subjected to 0.05 in. differential deflection for 90,000 cycles. Table 4.5 shows the configuration of these specimens that did not crack.

The common factor relating all of the specimens that cracked is that the membrane was placed directly on the deck surface and the hot-mix asphalt layers placed on the membrane. Membranes appear to act like an adhesive for the asphalt and glulam deck which more effectively reduces the length over which the asphalt layer is strained by the interpanel deck deflection. The bond between the asphalt layer and the glulam deck was broken on all of the uncracked test specimens. Debonding of the asphalt from deck probably allowed the strain to be relieved by increasing the length of asphalt over which the strain was distributed by creating a slight back-and-forth movement of the asphalt across the surface of the glulam deck panel. This in itself is not a concern unless shoving of the asphalt layer on the bridge deck becomes a problem.

The thickness of each layer of asphalt did not influence the results within the limits of this study nor did the type of waterproofing membrane. Although these series of cracking tests are not all inclusive, they do indicate the best placement of the membrane is between the two layers of asphalt in order to alleviate asphalt cracking caused by interpanel differential deflection. A configuration of a glulam deck panel, a hot-mix asphalt base layer, a waterproofing membrane, and a hot-mix asphalt surface layer is able to withstand repeated interpanel differential deflections of 0.05 in. without cracking and could be the optimal choice for ensuring the longevity of timber bridge wearing surfaces.

Table 4.5 Configuration of Uncracked Test Specimens

TEST DESIGNATION	CONFIGURATION
Specimen 3	3 in. of base mix asphalt layer placed on deck, 1-1/4 in. of surface mix asphalt layer placed on top
Specimen 4a	3 in. of base mix asphalt layer placed on deck, 1-1/4 in. of surface mix asphalt layer placed on top, Bituthene membrane placed between asphalt layers
Specimen 4b	3 in. of base mix asphalt layer placed on deck, 1-1/4 in. of surface mix asphalt layer placed on top, Petrotac membrane placed between asphalt layers
Specimen 4c	3 in. of base mix asphalt layer placed on deck, 1-1/4 in. of surface mix asphalt layer placed on top, Protectowrap membrane placed between asphalt layers
Specimen 5	1-1/2 in. of base mix asphalt layer placed on deck, 1 in. of surface mix asphalt layer placed on top
Specimen 6a	1-1/2 in. of base mix asphalt layer placed on deck, 1 in. of surface mix asphalt layer placed on top, Bituthene membrane placed between asphalt layers
Specimen 6b	1-1/2 in. of base mix asphalt layer placed on deck, 1 in. of surface mix asphalt layer placed on top, Petrotac membrane placed between asphalt layers
Specimen 6c	1-1/2 in. of base mix asphalt layer placed on deck, 1 in. of surface mix asphalt layer placed on top, Protectowrap membrane placed between asphalt layers

CHAPTER V

PROPOSED DESIGN CALCULATIONS

5.1 BACKGROUND

There appears to be no published procedures for the analysis and prediction of interpanel differential deflection of glulam deck panels on girder bridges. Current deck deflection design practice is to check the thickness of the deck and the span between girders against a chart derived from research and field observations for noninterconnected decks (Ritter, 1992). For interconnected decks, i.e. decks connected with steel dowels, it is assumed the deck acts as an orthotropic plate and that there are no significant interpanel differential deflections. The dowels must fit very snugly and remain so throughout the life of the deck for this to be true. Wood, by its very nature, will relax against mechanical pressure so the dowels will loosen over time because of this phenomenon. Wood also shrinks and swells with varying moisture content and this action will cause the dowels to loosen over time. Hence, it is recommended that interconnected deck panels not be treated as orthotropic plates and the potential interpanel differential deflection be examined.

5.2 PROPOSED DECK DEFLECTION MODEL

The focus of the deck deflection model is the interpanel differential deck deflection, and that is why contributing factors to the overall global deflections such as self weight and the weight of the wearing surface can be ignored. For the same reason, the deflection of the girders, e.g. the deck panel supports, do not affect the interpanel deflection. The experimental tests indicated the deck panel deforms in a similar manner to a beam and not as a plate.

Due to the fact that the span-to-depth ratio of the deck panels will be relatively low, shear deflection must be taken into consideration. Therefore the Mindlin/Timoshenko model for a beam will be used. This model assumes that although plane sections through the beam still remain straight and undeformed, they are not necessarily normal to the centroidal axis, this model allows consideration for shear deflection.

A typical deck panel on a glulam girder bridge may have four or more spans depending on the width of the bridge and load requirements of the bridge. A three span continuous beam is used for the model since additional spans will have little effect on the

deflection under consideration. It is sagacious to be conservative in a design or analysis of this nature, so the AASHTO truck loading can be assumed as a point load instead of a distributed load radiating out from the tire footprint. For the same reason, it is conservative to place two point loads (wheels) in the center of each outside span. The outside span is chosen because it is the most flexible of the spans and would have the greatest deflection, hence, it is the most conservative. These two assumptions are countered by the possibility that the dynamic loading of a passing vehicle can cause a slight rebound effect in the glulam deck panels. This rebound is the effect a load causes when it initially has caused a deflection in a panel and then quickly moves to an adjacent panel, the first panel tries to spring back toward its original shape and could do so with enough momentum to pass through the initial undeformed state and create a larger differential deflection.

The following equation for the deflection due to flexure of a three span continuous beam was derived in Section 3.2.3 (Equation 3.13).

$$y_b = \frac{1}{EI}\left[0.07083Px^3 - \frac{1}{6}P\left\langle x - \frac{L}{2}\right\rangle^3 + 0.09583P\langle x - L\rangle^3 + 0.09583P\langle x - 2L\rangle^3 - \frac{1}{6}P\left\langle x - \frac{5L}{2}\right\rangle^3 - 0.05PL^2x\right] \quad \textbf{(5.1)}$$

If the aforementioned assumption that the load is applied at the center of an outside span (i.e. $x = \frac{5L}{2}$) is made, then the equation for deflection due to flexure simplifies to

$$y_b = 0.01621\frac{PL^3}{EI} \quad \textbf{(5.2)}$$

An equation for deflection under the load (applied at the center of an outside span) due to shear for a three span continuous beam was given in Section 3.2.3 (Equation 3.14).

$$y_v = \frac{1}{2}\frac{E}{G}\left(\frac{d}{L}\right)^2 y_b \quad \textbf{(5.3)}$$

The final expression for the total deflection of a three span continuous beam with a point load applied at mid-span of one of the outside spans is determined by combining Equation 5.2 and Equation 5.3. If the assumption that $\frac{E}{G} = 16$ is made, the equation can be written as

$$y = \frac{1}{EI}\left(0.016PL^3 + 0.123d^2PL\right) \quad \textbf{(5.4)}$$

Where E is the modulus of elasticity of the glulam deck panel, I is the moment of inertia, P is the applied point load, L is the span length, and d is the depth (thickness) of the deck. Equation 5.4 may be used to estimate the maximum interpanel differential deck

deflection of a glulam deck girder bridge. A sample calculation is provided in Appendix C.

5.3 LIMITATIONS

The proposed design method for determining the interpanel differential deck deflection of a girder bridge is subject to the following limitations:

- Deck thickness used in most highway bridges allow the deck to be modeled as a beam instead of a plate. If thinner deck panels are used, the design may become too conservative.
- The ratio of the modulus of elasticity to the modulus of rigidity (E/G) is approximately 16. A ratio greater than 16 could provide less conservative results.
- Vehicular wheel load can be conservatively modeled as a point load.
- Load is applied at mid-span of the two outside spans of a three span continuous beam.
- Any effect due to dynamic rebounding is assumed to be negligible.

These assumptions are representative of most if not all glulam bridge decks. However, even with the above limitations, the proposed design method is a simple but useful method that designers of girder bridges with glulam decks may use to estimate the interpanel differential deflection.

CHAPTER VI

CONCLUSIONS

6.1 OBSERVATIONS

The comparison of the results from the experimental and analytical investigations and the review of current literature have resulted in the following observations:

- There is currently no published design method for calculating the interpanel differential deflection of glued laminated deck panels for girder bridges.
- A three span continuous beam is a good model for estimating the interpanel differential deflection of glued laminated deck panels.
- An acceptable expression for the interpanel differential deflection, that includes both flexural and shear deflection, is:

$$y = \frac{1}{EI}\left(0.01621PL^3 + 0.12968d^2PL\right)$$

- With a correct wearing surface configuration, 0.05 in. interpanel differential deck deflection is an acceptable level to prevent premature cracking of the wearing surface along lines of intersection of deck panels.

- The optimum wearing surface configuration for a glued laminated bridge deck appears to be a waterproofing membrane sandwiched between a base layer of hot-mix asphalt and a surface layer of hot-mix asphalt.

6.2 RECOMMENDATIONS

The following recommendations should be considered in the construction of any new timber bridge deck. They may also be applicable to longitudinal glulam bridges and stress laminated bridges.

- Waterproofing or geotextile membranes should not be applied directly to the wooden deck. This is contrary to published design guides.
- Waterproofing membranes should be placed between a hot-mix asphalt base and a hot-mix asphalt surface.
- Estimated maximum interpanel differential deflection should be limited to 0.05 in.

Both the base and surface hot-mix asphalt layer should be sloped to provide positive drainage. Care must be taken when detailing the membrane extremities to ensure an optimum waterproofing envelope for the bridge deck.

6.3 FUTURE RESEARCH NEEDS

The limited amount of information available for the determination of acceptable interpanel differential deflection indicates that there is a need for additional research. A research program involving field testing of a large number of bridges with regards to interpanel differential deflection should be considered. Additional laboratory tests should be performed with larger samples, perhaps a three span arrangement, to verify asphalt cracking results. Research should be directed toward verifying and establishing a design procedure that would ensure longevity of glulam bridge decks on girder bridges.

REFERENCES

Asphalt Institute (1983). *Asphalt Technology and Construction Practices - Instructors Guide*, Asphalt Institute, College Park, MD.

Davalos, J.F. and Salim, H.A. (1995). "Local deck effects in stress-laminated T-system timber bridges." *Structural Engineering Review*, 7(4), 267-276.

Dimakis, A. and Oliva, M.G. (1988). "Behavior of stress-laminated timber highway bridge." *Journal of Structural Engineering*, 114(8), 1850-1869.

Gutkowski, R.M. and McCutcheon, W.J. (1987). "Comparative performance of timber bridges." *Journal of Structural Engineering*, 113(7), 1468-1486.

Haramis, J.E. (1997). "Investigation of bond strength and watertightness of waterproof asphalt concrete wearing surfaces for timber bridge decks." M.S. thesis, Virginia Polytechnic Institute and State University, Blacksburg, Virginia.

Habibullah, A. and Wilson, E.L. (1992). *SAP90 Structural Analysis Users Manual*, Computers and Structures, Inc., Berkley, California.

Ritter, M.A. (1992). *Timber Bridges: Design, Construction, Inspection, and Maintenance*, United States Department of Agriculture, Washington, District of Columbia.

Williamson, T.G. (1990). "Glued laminated timber for bridge construction." Serviceability and Durability of Construction Materials - Proceedings of the First Materials Engineering Congress Part 1, ASCE, Denver, Colorado.

Wipf, T.J., Klaiber, F.W., and Funke, R.W. (1990). "Longitudinal glued laminated timber bridge modeling." *Journal of Structural Engineering*, 116(4), 1121-1134.

APPENDIX A
TEST SUMMARY SHEETS

This appendix contains the test summary sheets for the experimental deflection tests. The test designations are Panel 1 through Panel 16 and the test matrix can be found in Table 2.1. There were two thickness of the deck panels tested, 5-1/8 in and 6-3/4 in, and both had dimensions of 48 in by 168 in. The simple beam configuration had a single span of 144 in while the continuous beam configuration had a three equal spans of 48 in. The test configurations are shown in Figure 2.1. Two types of boundary conditions were used in the deflection tests, knife-edge and bracket clips. The knife edge supports were fabricated from 1/4 in plate and angle. A 1 x 1 x 1/4 in angle was welded with the angle legs down to a 4 in by 48 in 1/4 in plate, a second 4 in by 48 in 1/4 in plate was placed on top of the angle and was temporarily supported until the test specimen was placed on the fabricated knife-edge. The bracket supports were the cast aluminum mounting brackets developed by the Weyerhaeuser Company for use on glulam bridge decks. They were mounted to the deck by carriage bolts and were fitted into routed grooves in the supporting "girders." The test results include a recorded test load and associated deflection for the simple beam and a point from the linear regression of the average of the deflections of the continuous beam and associated deflection. The effective modulus of elasticity calculated from classical analysis equations. The deck panels were not loaded to failure and the deflections were kept small to ensure linear elastic behavior.

APPENDIX A
TEST SUMMARY SHEETS

Test Designation		Page
Panel 1	One span with knife-edge supports	60
Panel 2	Three span with knife-edge supports	62
Panel 3	Three span with clip supports	64
Panel 4	One span with clip supports	66
Panel 5	One span with knife-edge supports	68
Panel 6	Three span with knife-edge supports	70
Panel 7	Three span with clip supports	72
Panel 8	One span with clip supports	74
Panel 9	One span with knife-edge supports	76
Panel 10	Three span with knife-edge supports	78
Panel 11	Three span with clip supports	80
Panel 12	One span with clip supports	82
Panel 13	One span with knife-edge supports	84
Panel 14	Three span with knife-edge supports	86
Panel 15	Three span with clip supports	88
Panel 16	One span with clip supports	90

TEST NAME: Panel 1
TEST DATE: July, 1995
PURPOSE: Load deformation characteristics

TEST DESCRIPTION

Number of spans:	one
Type of boundary supports	knife-edge
Span length	144 in
Deck panel width	48 in
Deck panel depth	5-1/8 in
Cross-sectional area	246 in^2
Moment of inertia	538 in^4
Specimen	SYP Glulam

TEST RESULTS

Load	30.1 kips
Deflection	1.43 in
Effective modulus of elasticity	2,400,000 psi

Panel 1
Load vs. Deflection

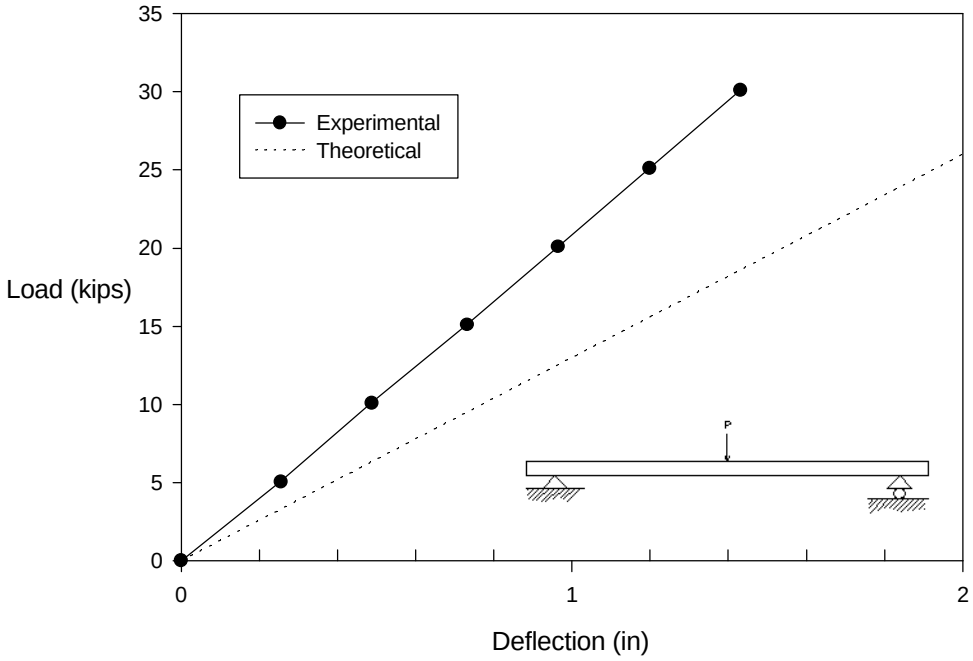

TEST NAME: Panel 2
TEST DATE: July, 1995
PURPOSE: Load deformation characteristics

TEST DESCRIPTION

Number of spans:	three
Type of boundary supports	knife-edge
Span length	48 in
Deck panel width	48 in
Deck panel depth	5-1/8 in
Cross-sectional area	246 in^2
Moment of inertia	538 in^4
Specimen	SYP Glulam

TEST RESULTS

Load	28.0 kips
Deflection	0.05 in
Effective modulus of elasticity	2,000,000 psi

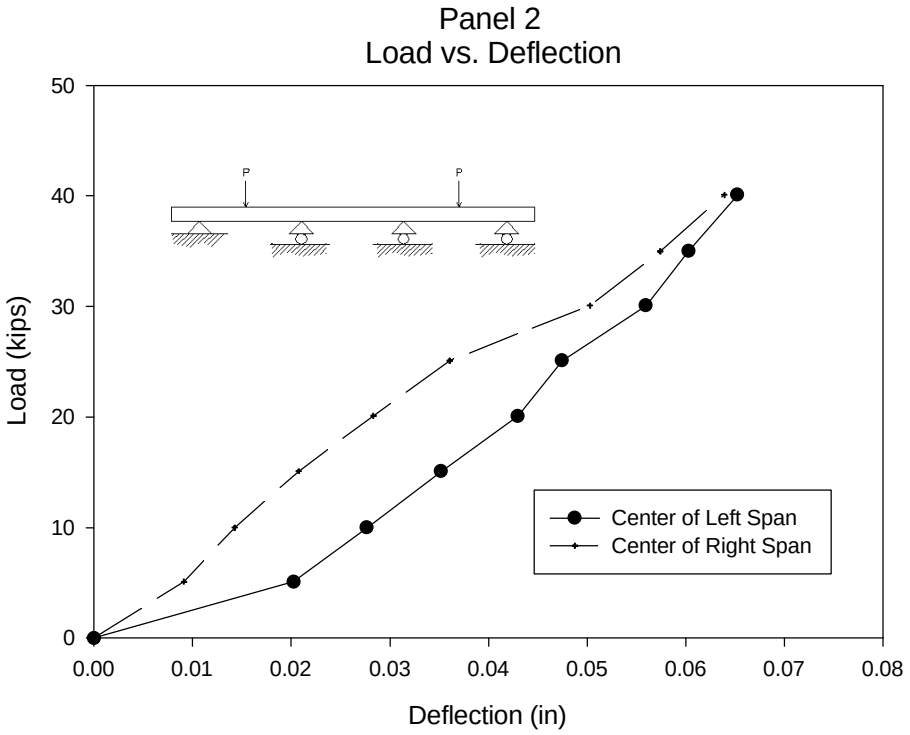
Panel 2
Load vs. Deflection
Load (kips)
Deflection (in)
P
P
Center of Left Span
Center of Right Span
0
10
20
30
40
50
0.00
0.01
0.02
0.03
0.04
0.05
0.06
0.07
0.08

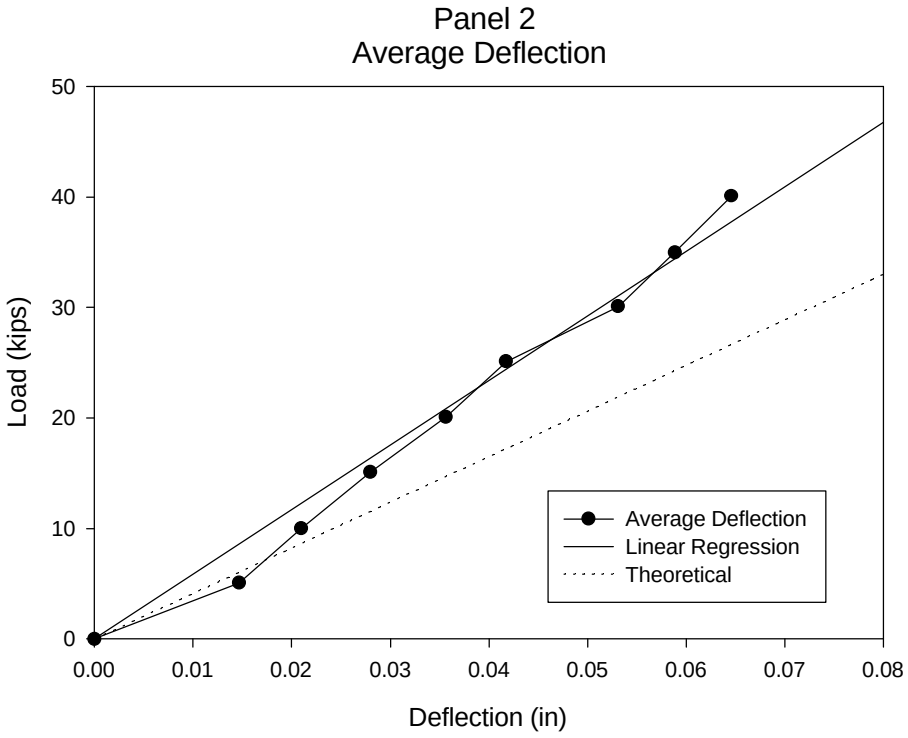
Panel 2
Average Deflection
Load (kips)
Deflection (in)
Average Deflection
Linear Regression
Theoretical
0
10
20
30
40
50
0.00
0.01
0.02
0.03
0.04
0.05
0.06
0.07
0.08

TEST NAME: Panel 3
TEST DATE: July, 1995
PURPOSE: Load deformation characteristics

TEST DESCRIPTION

Number of spans:	three
Type of boundary supports	bracket clips
Span length	48 in
Deck panel width	48 in
Deck panel depth	5-1/8 in
Cross-sectional area	246 in^2
Moment of inertia	538 in^4
Specimen	SYP Glulam

TEST RESULTS

Load	30.0 kips
Deflection	0.053 in
Effective modulus of elasticity	2,100,000 psi

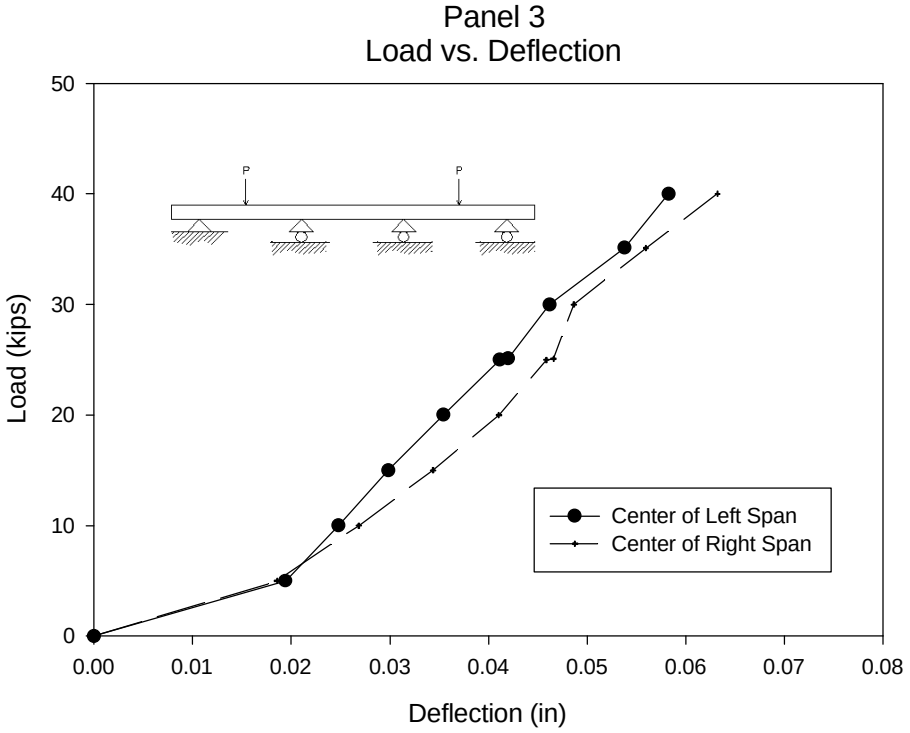
Panel 3
Load vs. Deflection
P
P
Load (kips)
Deflection (in)
Center of Left Span
Center of Right Span
0
10
20
30
40
50
0.00
0.01
0.02
0.03
0.04
0.05
0.06
0.07
0.08

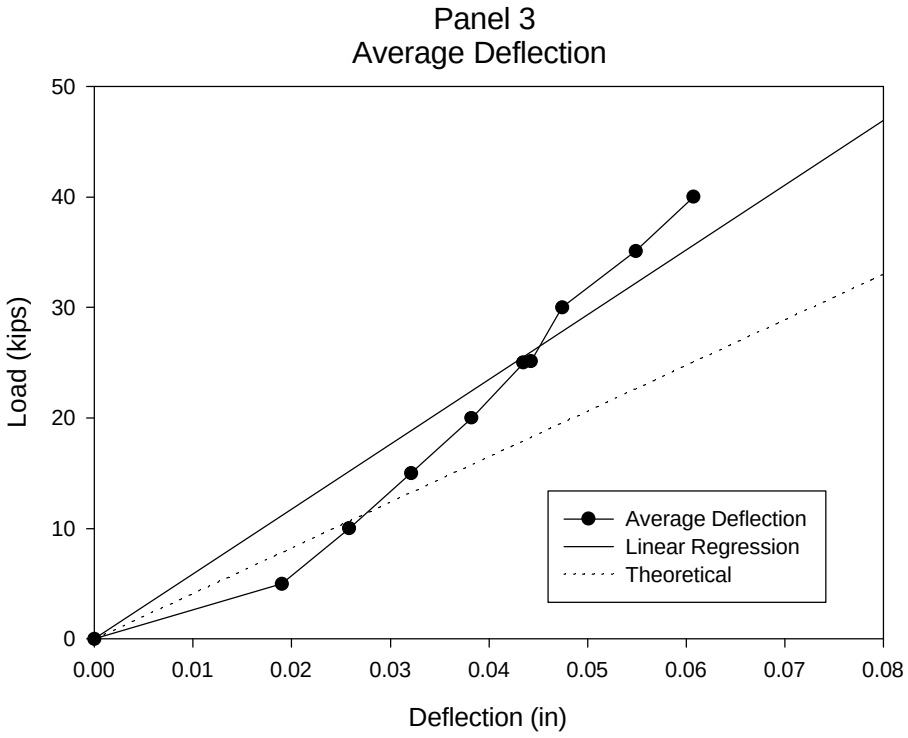
Panel 3
Average Deflection
Load (kips)
Deflection (in)
Average Deflection
Linear Regression
Theoretical
0
10
20
30
40
50
0.00
0.01
0.02
0.03
0.04
0.05
0.06
0.07
0.08

TEST NAME: Panel 4
TEST DATE: July, 1995
PURPOSE: Load deformation characteristics

TEST DESCRIPTION

Number of spans:	one
Type of boundary supports	bracket clips
Span length	144 in
Deck panel width	48 in
Deck panel depth	5-1/8 in
Cross-sectional area	246 in^2
Moment of inertia	538 in^4
Specimen	SYP Glulam

TEST RESULTS

Load	30.1 kips
Deflection	1.31 in
Effective modulus of elasticity	2,600,000 psi

Panel 4
Load vs. Deflection

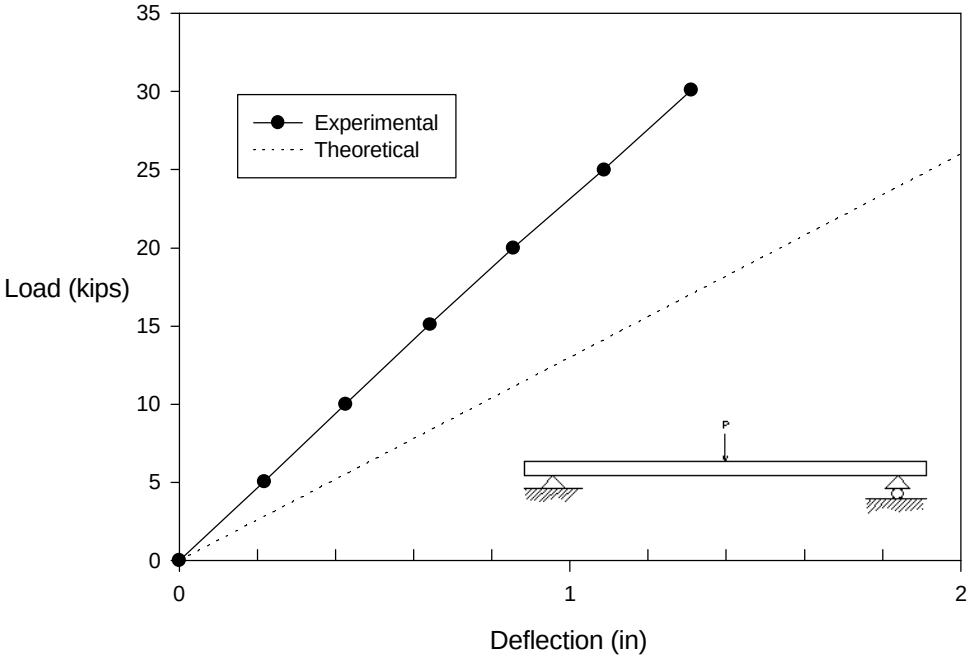

TEST NAME: Panel 5
TEST DATE: July, 1995
PURPOSE: Load deformation characteristics

TEST DESCRIPTION

Number of spans:	one
Type of boundary supports	knife-edge
Span length	144 in
Deck panel width	48 in
Deck panel depth	5-1/8 in
Cross-sectional area	246 in^2
Moment of inertia	538 in^4
Specimen	SYP Glulam

TEST RESULTS

Load	30.0 kips
Deflection	1.55 in
Effective modulus of elasticity	2,200,000 psi

Panel 5
Load vs. Deflection

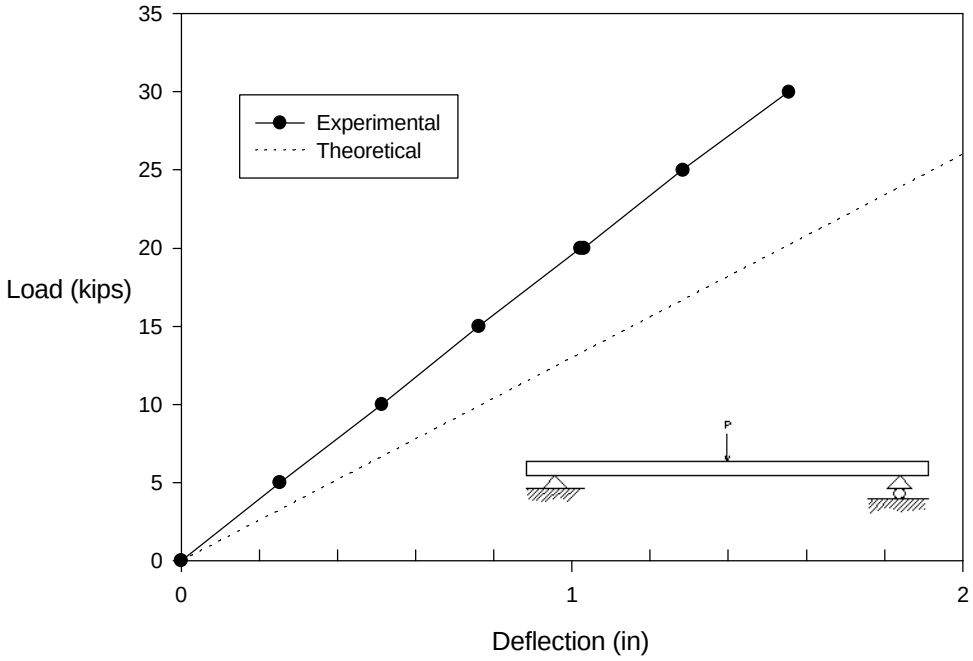

TEST NAME: Panel 6
TEST DATE: July, 1995
PURPOSE: Load deformation characteristics

TEST DESCRIPTION

Number of spans:	three
Type of boundary supports	knife-edge
Span length	48 in
Deck panel width	48 in
Deck panel depth	5-1/8 in
Cross-sectional area	246 in^2
Moment of inertia	538 in^4
Specimen	SYP Glulam

TEST RESULTS

Load	32.0 kips
Deflection	0.05 in
Effective modulus of elasticity	2,300,000 psi

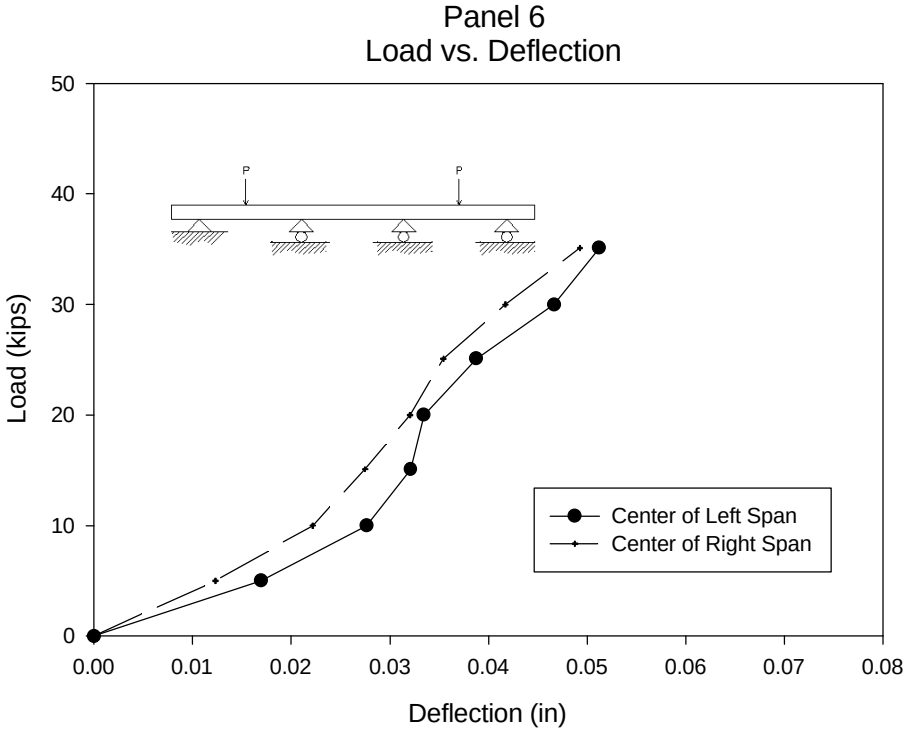
Panel 6
Load vs. Deflection
Load (kips)
Deflection (in)
P
P
Center of Left Span
Center of Right Span
0
10
20
30
40
50
0.00
0.01
0.02
0.03
0.04
0.05
0.06
0.07
0.08

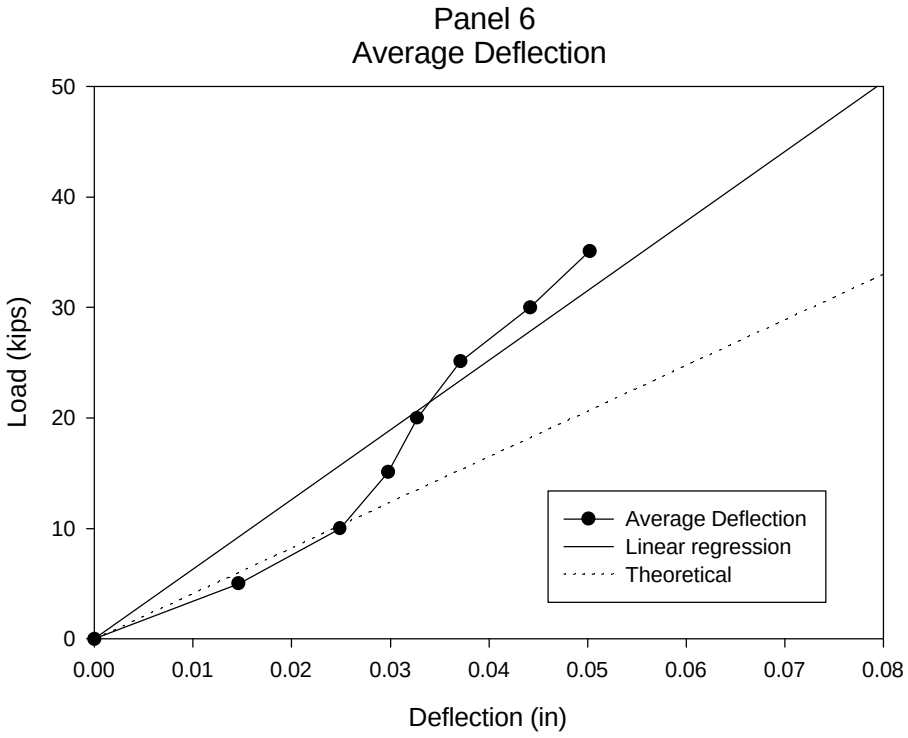
Panel 6
Average Deflection
Load (kips)
Deflection (in)
Average Deflection
Linear regression
Theoretical
0
10
20
30
40
50
0.00
0.01
0.02
0.03
0.04
0.05
0.06
0.07
0.08

TEST NAME: Panel 7
TEST DATE: July, 1995
PURPOSE: Load deformation characteristics

TEST DESCRIPTION

Number of spans:	three
Type of boundary supports	bracket clips
Span length	48 in
Deck panel width	48 in
Deck panel depth	5-1/8 in
Cross-sectional area	246 in^2
Moment of inertia	538 in^4
Specimen	SYP Glulam

TEST RESULTS

Load	27.0 kips
Deflection	0.04 in
Effective modulus of elasticity	2,400,000 psi

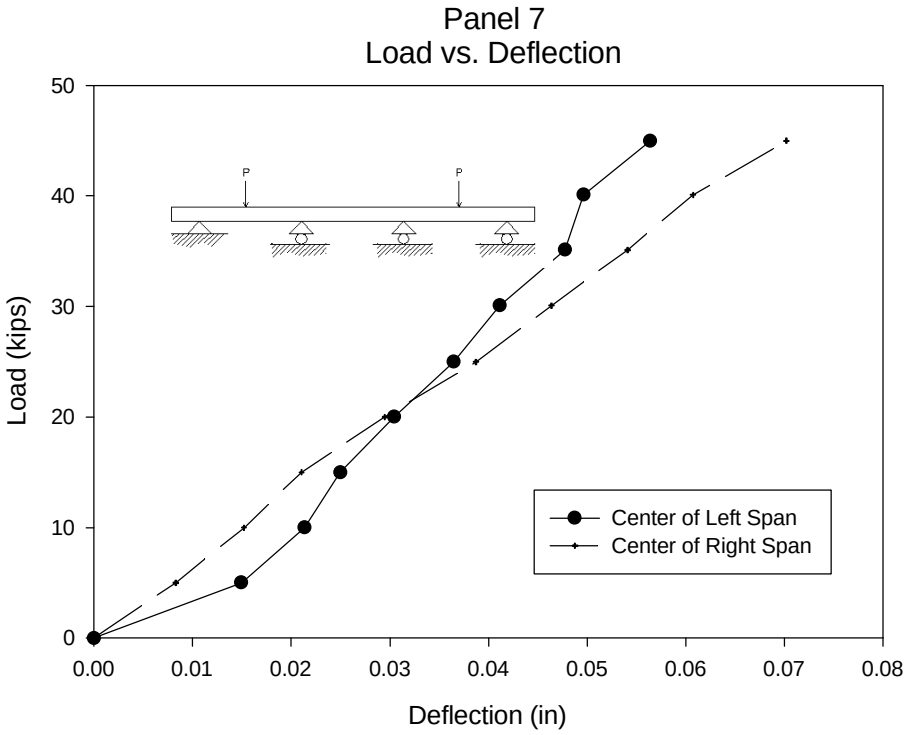
Panel 7
Load vs. Deflection
Load (kips)
Deflection (in)
P
P
Center of Left Span
Center of Right Span
0
10
20
30
40
50
0.00
0.01
0.02
0.03
0.04
0.05
0.06
0.07
0.08

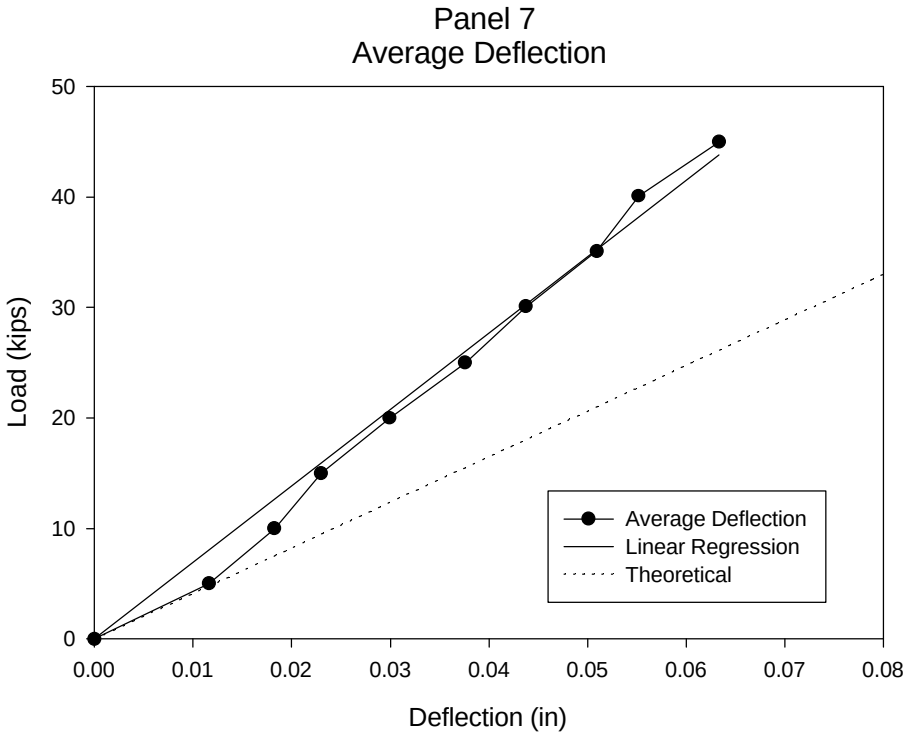
Panel 7
Average Deflection
Load (kips)
Deflection (in)
Average Deflection
Linear Regression
Theoretical
0
10
20
30
40
50
0.00
0.01
0.02
0.03
0.04
0.05
0.06
0.07
0.08

TEST NAME: Panel 8
TEST DATE: July, 1995
PURPOSE: Load deformation characteristics

TEST DESCRIPTION

Number of spans:	one
Type of boundary supports	bracket clips
Span length	144 in
Deck panel width	48 in
Deck panel depth	5-1/8 in
Cross-sectional area	246 in^2
Moment of inertia	538 in^4
Specimen	SYP Glulam

TEST RESULTS

Load	30.0 kips
Deflection	1.43 in
Effective modulus of elasticity	2,400,000 psi

Panel 8
Load vs. Deflection

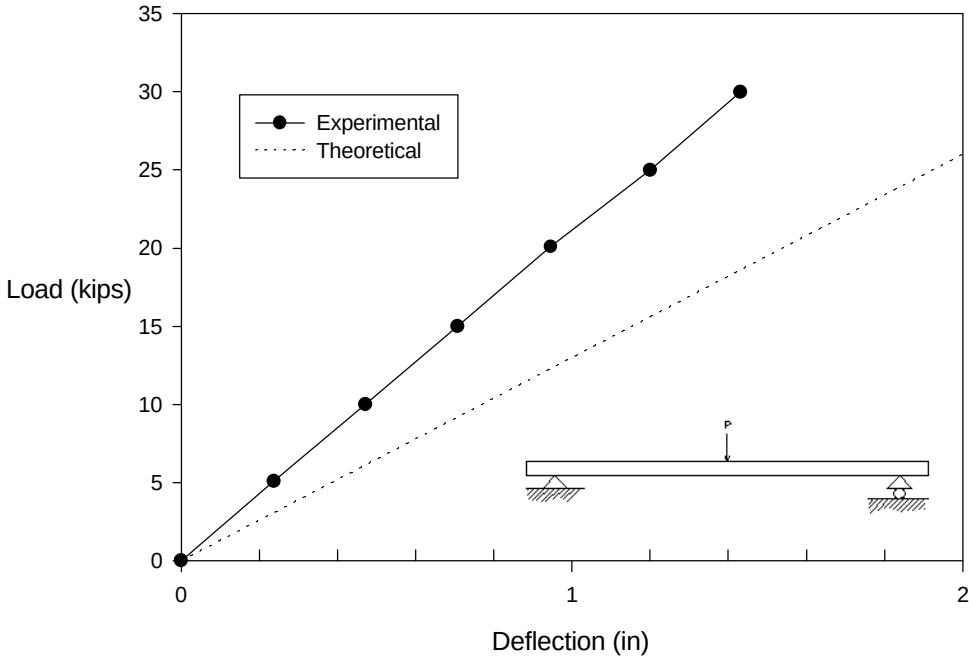

TEST NAME: Panel 9
TEST DATE: July, 1995
PURPOSE: Load deformation characteristics

TEST DESCRIPTION

Number of spans:	one
Type of boundary supports	knife-edge
Span length	144 in
Deck panel width	48 in
Deck panel depth	6-3/4 in
Cross-sectional area	324 in^2
Moment of inertia	1230 in^4
Specimen	SYP Glulam

TEST RESULTS

Load	30.1 kips
Deflection	0.85 in
Effective modulus of elasticity	1,800,000 psi

Panel 9
Load vs. Deflection

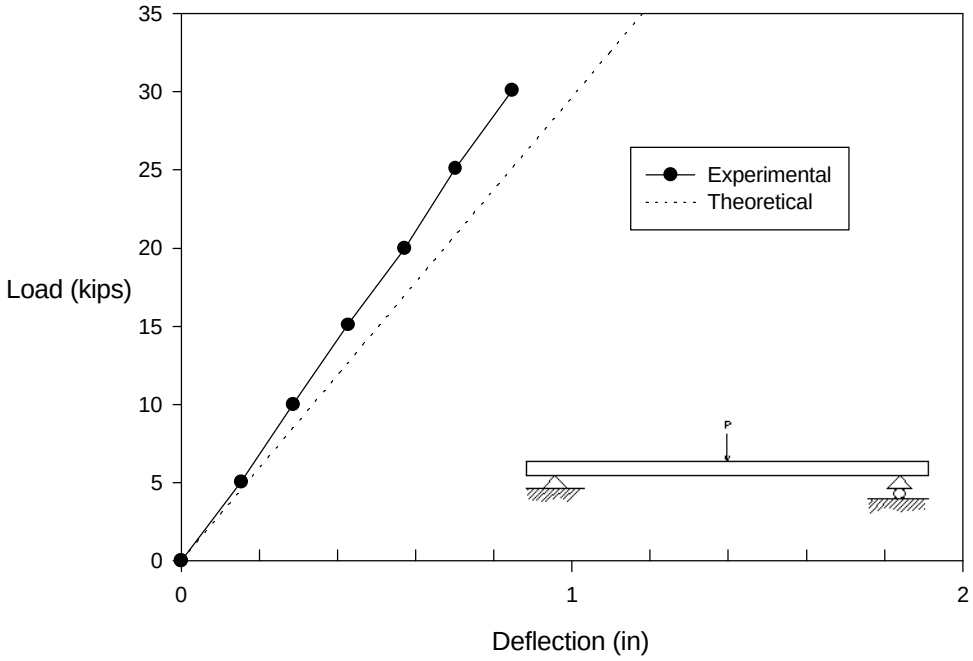

TEST NAME: Panel 10
TEST DATE: July, 1995
PURPOSE: Load deformation characteristics

TEST DESCRIPTION

Number of spans:	three
Type of boundary supports	knife-edge
Span length	48 in
Deck panel width	48 in
Deck panel depth	6-3/4 in
Cross-sectional area	324 in^2
Moment of inertia	1230 in^4
Specimen	SYP Glulam

TEST RESULTS

Load	30.0 kips
Deflection	0.04 in
Effective modulus of elasticity	1,400,000 psi

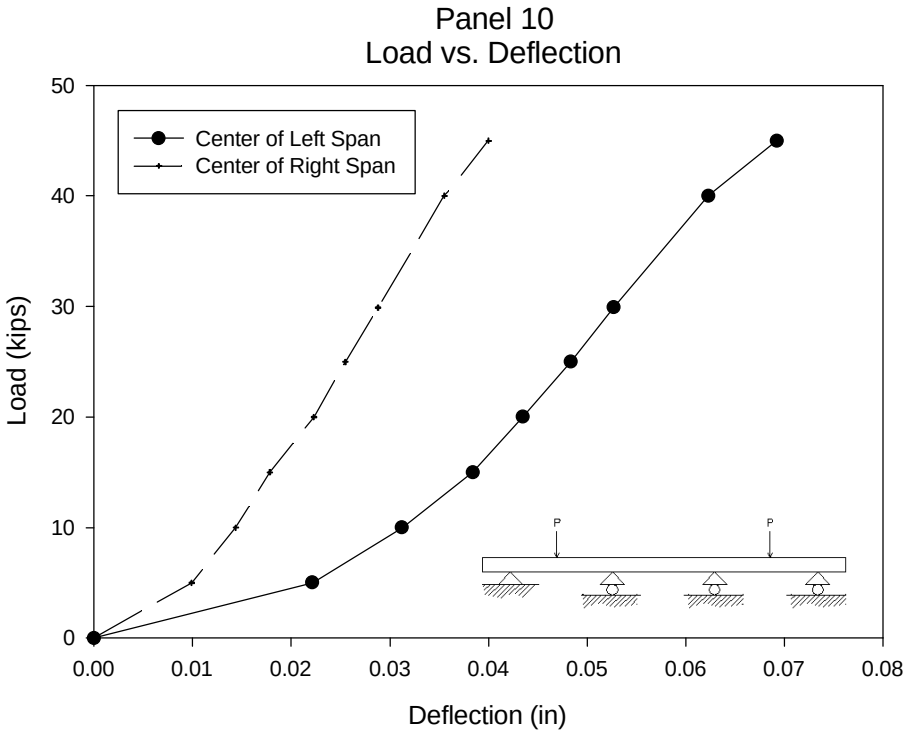
Panel 10
Load vs. Deflection
Center of Left Span
Center of Right Span
Load (kips)
Deflection (in)
0
10
20
30
40
50
0.00
0.01
0.02
0.03
0.04
0.05
0.06
0.07
0.08
P
P

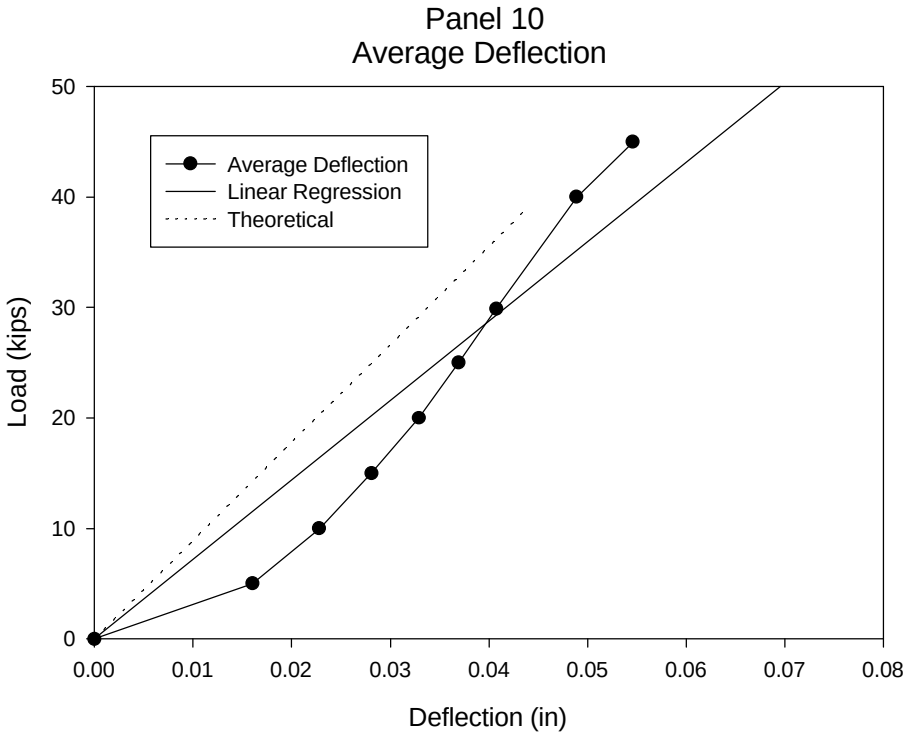
Panel 10
Average Deflection
Average Deflection
Linear Regression
Theoretical
Load (kips)
Deflection (in)
0
10
20
30
40
50
0.00
0.01
0.02
0.03
0.04
0.05
0.06
0.07
0.08

TEST NAME: Panel 11
TEST DATE: July, 1995
PURPOSE: Load deformation characteristics

TEST DESCRIPTION

Number of spans:	three
Type of boundary supports	bracket clips
Span length	48 in
Deck panel width	48 in
Deck panel depth	6-3/4 in
Cross-sectional area	324 in^2
Moment of inertia	1230 in^4
Specimen	SYP Glulam

TEST RESULTS

Load	30.0 kips
Deflection	0.037 in
Effective modulus of elasticity	1,500,000 psi

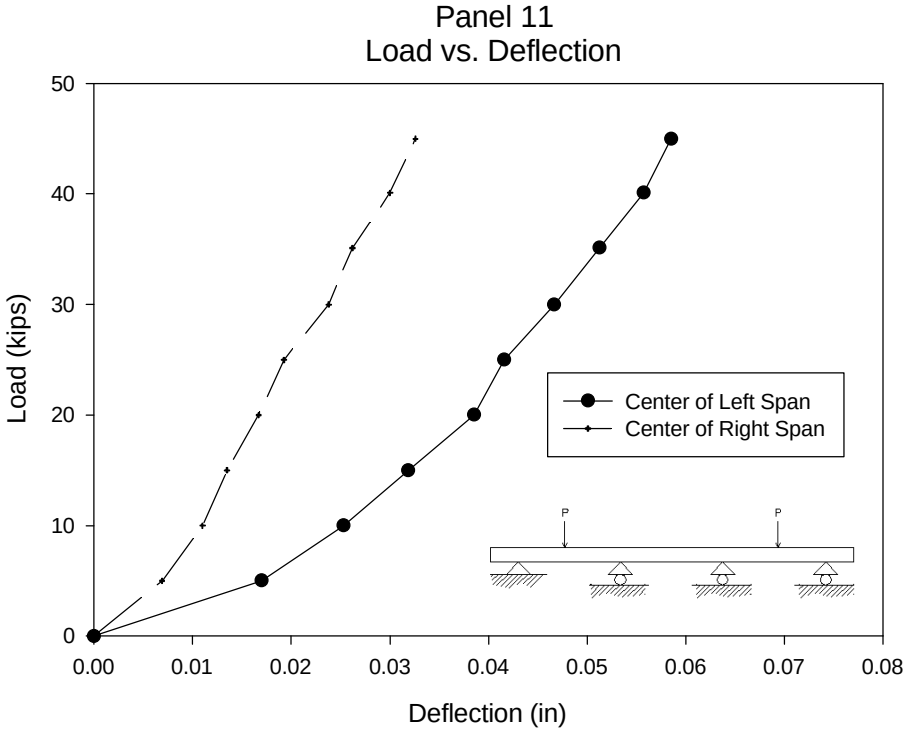
Panel 11
Load vs. Deflection
Load (kips)
Deflection (in)
Center of Left Span
Center of Right Span
P
P

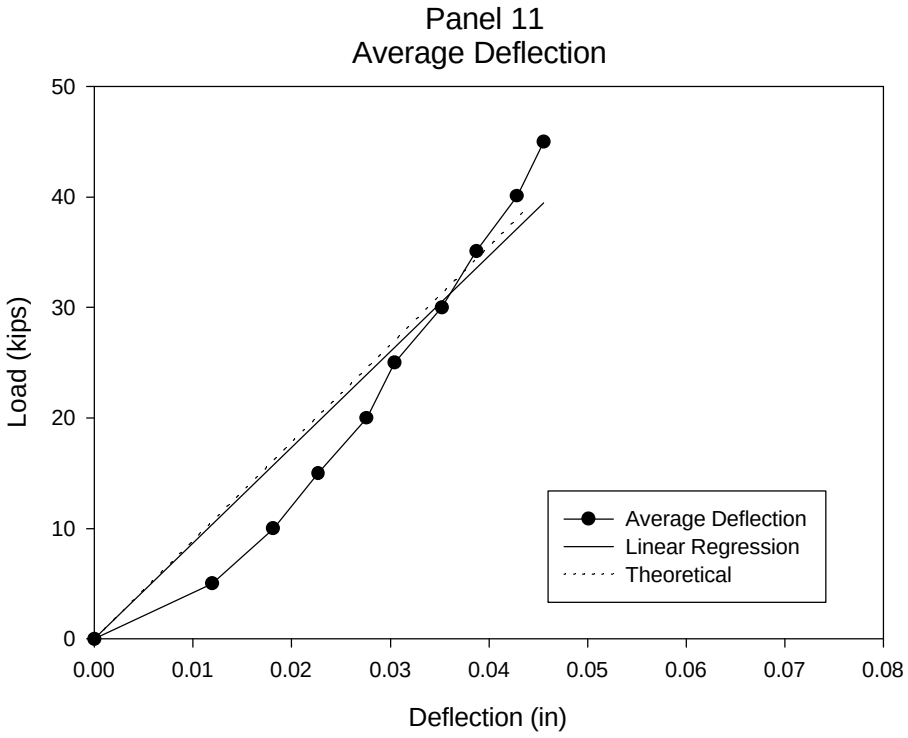
Panel 11
Average Deflection
Load (kips)
Deflection (in)
Average Deflection
Linear Regression
Theoretical

TEST NAME: Panel 12
TEST DATE: July, 1995
PURPOSE: Load deformation characteristics

TEST DESCRIPTION

Number of spans:	one
Type of boundary supports	bracket clips
Span length	144 in
Deck panel width	48 in
Deck panel depth	6-3/4 in
Cross-sectional area	324 in^2
Moment of inertia	1230 in^4
Specimen	SYP Glulam

TEST RESULTS

Load	40.0 kips
Deflection	1.07 in
Effective modulus of elasticity	1,900,000 psi

Panel 12
Load vs. Deflection

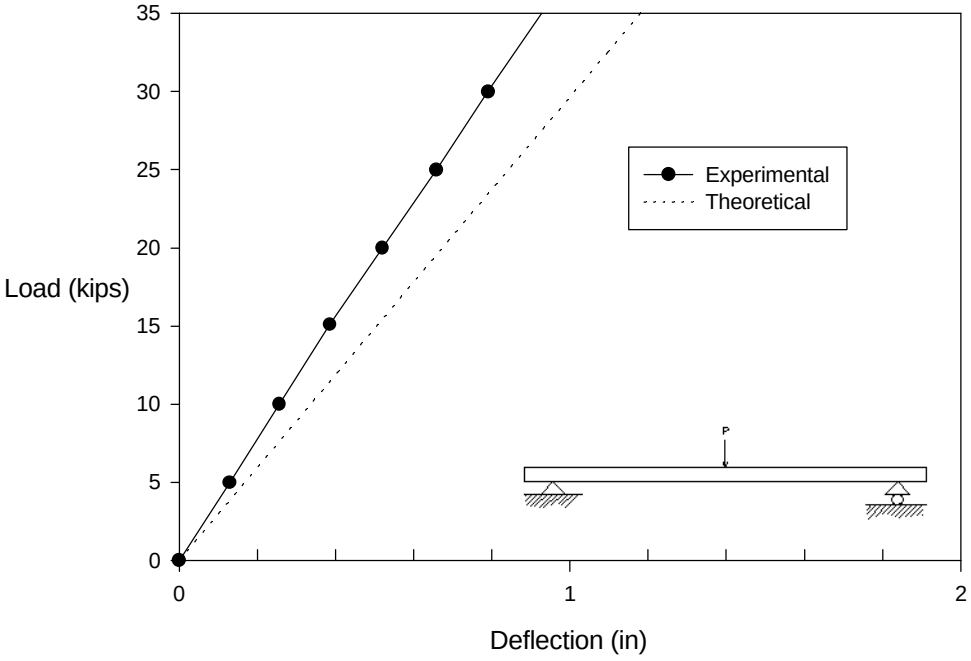

TEST NAME: Panel 13
TEST DATE: July, 1995
PURPOSE: Load deformation characteristics

TEST DESCRIPTION

Number of spans:	one
Type of boundary supports	knife-edge
Span length	144 in
Deck panel width	48 in
Deck panel depth	6-3/4 in
Cross-sectional area	324 in^2
Moment of inertia	1230 in^4
Specimen	SYP Glulam

TEST RESULTS

Load	40.0 kips
Deflection	0.061 in
Effective modulus of elasticity	1,700,000 psi

Panel 13
Load vs. Deflection

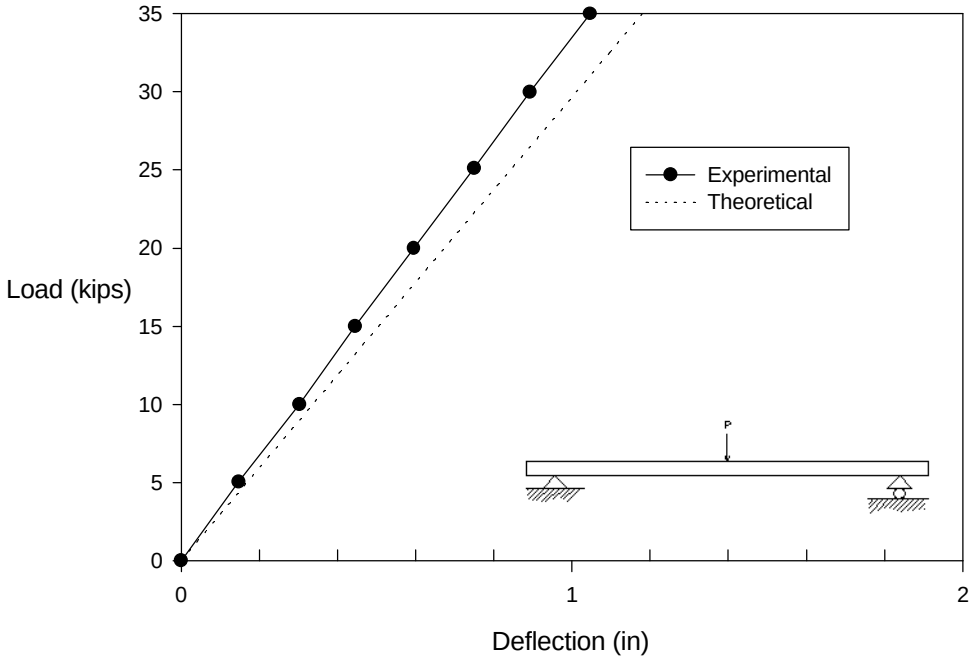

TEST NAME: Panel 14
TEST DATE: July, 1995
PURPOSE: Load deformation characteristics

TEST DESCRIPTION

Number of spans:	three
Type of boundary supports	knife-edge
Span length	48 in
Deck panel width	48 in
Deck panel depth	6-3/4 in
Cross-sectional area	324 in^2
Moment of inertia	1230 in^4
Specimen	SYP Glulam

TEST RESULTS

Load	35.0 kips
Deflection	0.05 in
Effective modulus of elasticity	1,200,000 psi

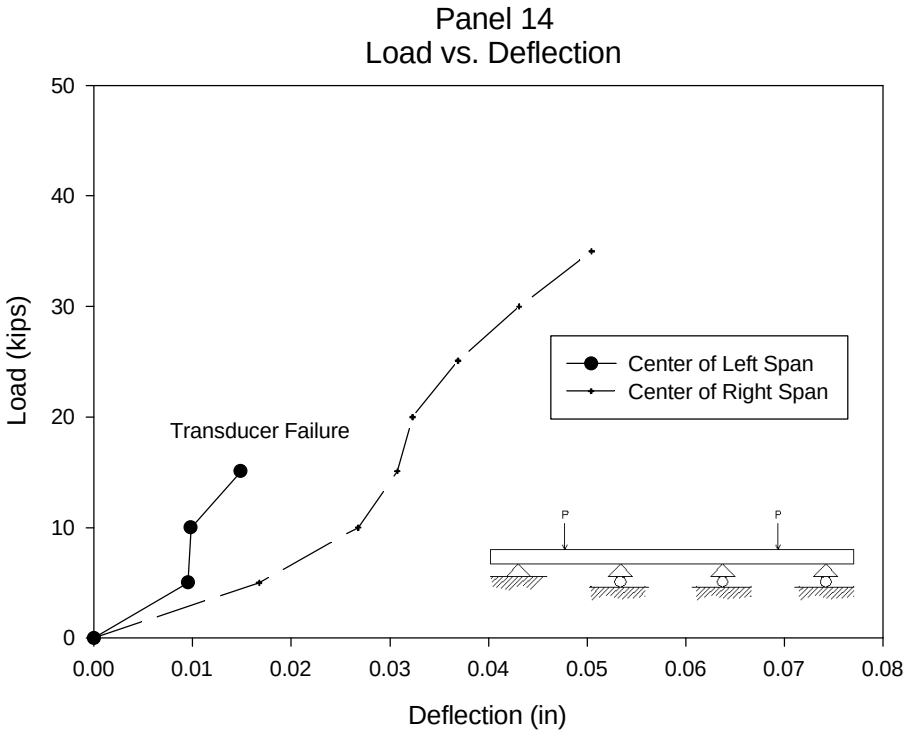
Panel 14
Load vs. Deflection
Load (kips)
Deflection (in)
Transducer Failure
Center of Left Span
Center of Right Span
P
P
0
10
20
30
40
50
0.00
0.01
0.02
0.03
0.04
0.05
0.06
0.07
0.08

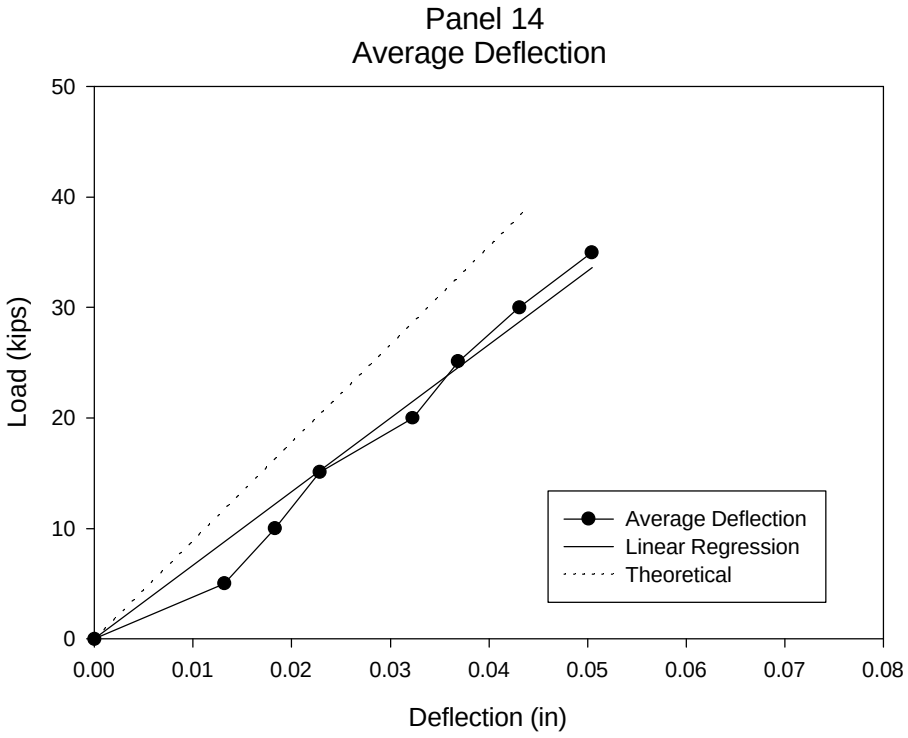
Panel 14
Average Deflection
Load (kips)
Deflection (in)
Average Deflection
Linear Regression
Theoretical
0
10
20
30
40
50
0.00
0.01
0.02
0.03
0.04
0.05
0.06
0.07
0.08

TEST NAME: Panel 15
TEST DATE: July, 1995
PURPOSE: Load deformation characteristics

TEST DESCRIPTION

Number of spans:	three
Type of boundary supports	bracket clips
Span length	48 in
Deck panel width	48 in
Deck panel depth	6-3/4 in
Cross-sectional area	324 in^2
Moment of inertia	1230 in^4
Specimen	SYP Glulam

TEST RESULTS

Load	30.0 kips
Deflection	0.034 in
Effective modulus of elasticity	1,500,000 psi

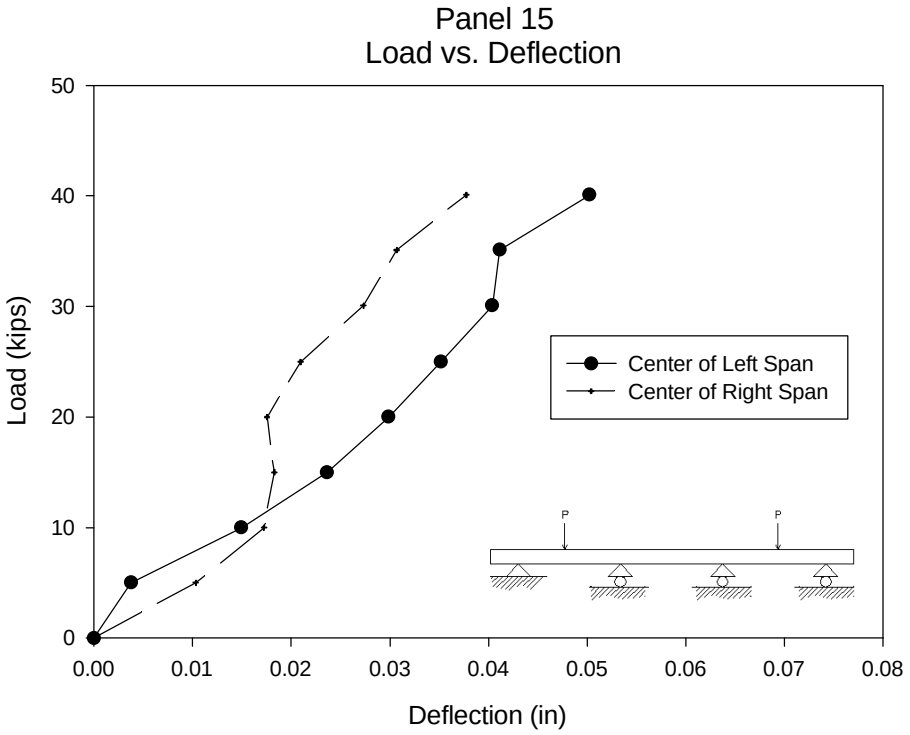
Panel 15
Load vs. Deflection
Load (kips)
Deflection (in)
0
10
20
30
40
50
0.00
0.01
0.02
0.03
0.04
0.05
0.06
0.07
0.08
Center of Left Span
Center of Right Span
P
P

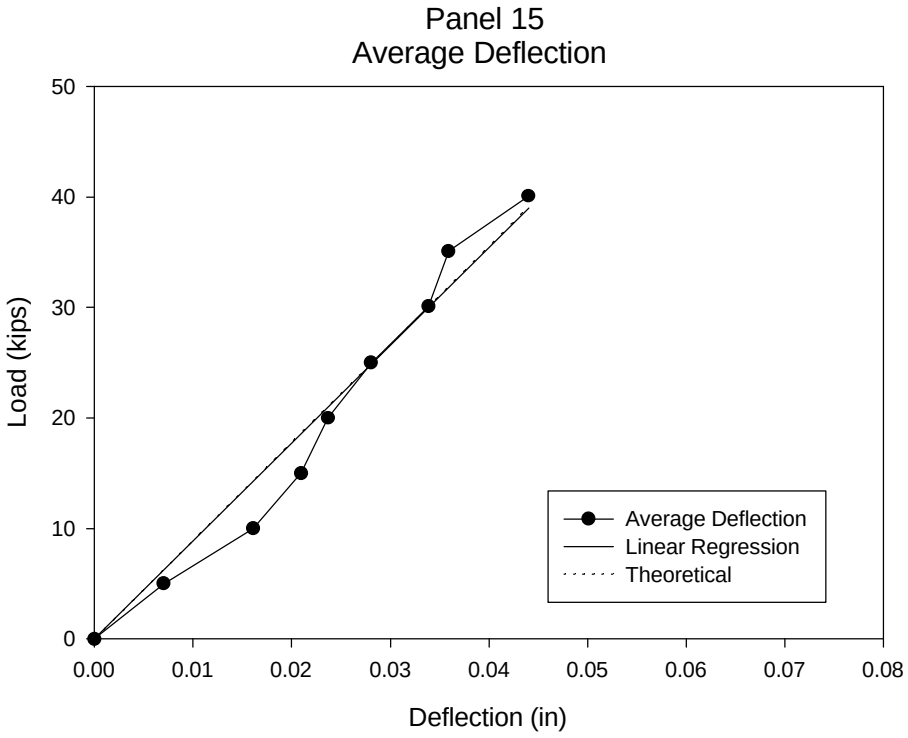
Panel 15
Average Deflection
Load (kips)
Deflection (in)
0
10
20
30
40
50
0.00
0.01
0.02
0.03
0.04
0.05
0.06
0.07
0.08
Average Deflection
Linear Regression
Theoretical

TEST NAME: Panel 16
TEST DATE: July, 1995
PURPOSE: Load deformation characteristics

TEST DESCRIPTION

Number of spans:	one
Type of boundary supports	bracket clips
Span length	144 in
Deck panel width	48 in
Deck panel depth	6-3/4 in
Cross-sectional area	324 in^2
Moment of inertia	1230 in^4
Specimen	SYP Glulam

TEST RESULTS

Load	30.0 kips
Deflection	0.82 in
Effective modulus of elasticity	1,800,000 psi

Panel 16
Load vs. Deflection

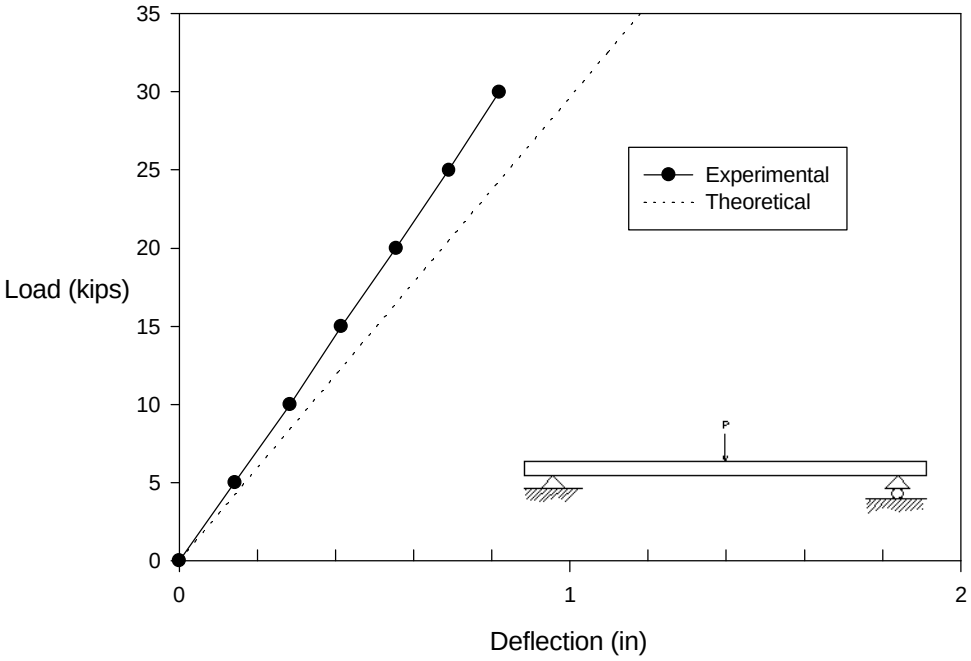

APPENDIX B

FINITE ELEMENT INPUT FILES

A finite element model of the experimental deck panels used in the deflection test was developed using shell elements in the commercial finite element program Sap90 (Wilson and Habibullah, 1995). The shell elements used were four node, isoparametric formulation including rotational stiffness components both in-plane and in the direction normal to the plane of the element. These elements include shear deflection in the the analysis of the total deflection. An eight point numerical integration scheme was used for the elements, and forces and moments were evaluated at the integration points and extrapolated to the joints of the element.

File Designation		Page
Ajoe1	Typical single span deflection model	93
Ajoe7	Typical three span deflection model	96

Typical Single Span Deflection Model - SAP90

```
C This is file AJOE1
C Units are KIP INCHES
SYSTEM
 R=0 L=1 C=0 V=0 T=0.0001 P=0 W=0 Z=0
GRID
 XN=13 YN=13 ZN=1
 0 12 24 36 48 60 72 84
 96 108 120 132 144
 0 4 8 12 16 20 24 28
 32 36 40 44 48
 0
JOINTS
 1       X=0  Y=0 Z=0
 2       X=12 Y=0 Z=0
 3       X=24 Y=0 Z=0
 4       X=36 Y=0 Z=0
 5       X=48 Y=0 Z=0
 6       X=60 Y=0 Z=0
 7       X=72 Y=0 Z=0
 8       X=84 Y=0 Z=0
 9       X=96 Y=0 Z=0
 10     X=108 Y=0 Z=0
 11     X=120 Y=0 Z=0
 12     X=132 Y=0 Z=0
 13     X=144 Y=0 Z=0
 14     X=0 Y=4 Z=0
 27     X=0 Y=8 Z=0
 40     X=0 Y=12 Z=0
 53     X=0 Y=16 Z=0
 66     X=0 Y=20 Z=0
 79     X=0 Y=24 Z=0
 92     X=0 Y=28 Z=0
 105    X=0 Y=32 Z=0
 118    X=0 Y=36 Z=0
 131    X=0 Y=40 Z=0
 144    X=0 Y=44 Z=0
 157    X=0 Y=48 Z=0
 1      X=0 Y=0 Z=0 F=1,12,12,1,13

SHELL
```

```
NM=1 O=0
1   E=1500 U=0.3 W=0.028935 M=0 TA=0
1      JQ=1,2,14,15 ETYPE=0 M=1 TZ=0 TH=5.125,5.125 LP=0 G=12,12

RESTRAINTS
 157  157  1    R=1,1,1,1,0,1
 144  144  1    R=1,1,1,1,0,1
 131  131  1    R=1,1,1,1,0,1
 118  118  1    R=1,1,1,1,0,1
 105  105  1    R=1,1,1,1,0,1
 92   92   1    R=1,1,1,1,0,1
 79   79   1    R=1,1,1,1,0,1
 66   66   1    R=1,1,1,1,0,1
 53   53   1    R=1,1,1,1,0,1
 40   40   1    R=1,1,1,1,0,1
 27   27   1    R=1,1,1,1,0,1
 14   14   1    R=1,1,1,1,0,1
 1    1    1    R=1,1,1,1,0,1
 169  169  1    R=0,1,1,1,0,1
 156  156  1    R=0,1,1,1,0,1
 143  143  1    R=0,1,1,1,0,1
 130  130  1    R=0,1,1,1,0,1
 117  117  1    R=0,1,1,1,0,1
 104  104  1    R=0,1,1,1,0,1
 91   91   1    R=0,1,1,1,0,1
 78   78   1    R=0,1,1,1,0,1
 65   65   1    R=0,1,1,1,0,1
 52   52   1    R=0,1,1,1,0,1
 39   39   1    R=0,1,1,1,0,1
 26   26   1    R=0,1,1,1,0,1
 13   13   1    R=0,1,1,1,0,1

LOADS
 163  163  1    L=1 F=0,0,-0.5,0,0,0
 150  150  1    L=1 F=0,0,-0.5,0,0,0
 137  137  1    L=1 F=0,0,-0.5,0,0,0
 124  124  1    L=1 F=0,0,-0.5,0,0,0
 111  111  1    L=1 F=0,0,-0.5,0,0,0
 98   98   1    L=1 F=0,0,-0.5,0,0,0
 85   85   1    L=1 F=0,0,-0.5,0,0,0
 72   72   1    L=1 F=0,0,-0.5,0,0,0
 59   59   1    L=1 F=0,0,-0.5,0,0,0
 46   46   1    L=1 F=0,0,-0.5,0,0,0
```

33 33 1 L=1 F=0,0,-0.5,0,0,0
20 20 1 L=1 F=0,0,-0.5,0,0,0
7 7 1 L=1 F=0,0,-0.5,0,0,0

Typical Three Span Deflection Model - SAP90

```
C This is file AJOE7
C Units are KIP INCHES
SYSTEM
 R=0 L=1 C=0 V=0 T=0.0001 P=0 W=0 Z=0
GRID
 XN=13 YN=13 ZN=1
 0 12 24 36 48 60 72 84
 96 108 120 132 144
 0 4 8 12 16 20 24 28
 32 36 40 44 48
 0
JOINTS
 1      X=0 Y=0 Z=0
 2      X=12 Y=0 Z=0
 3      X=24 Y=0 Z=0
 4      X=36 Y=0 Z=0
 5      X=48 Y=0 Z=0
 6      X=60 Y=0 Z=0
 7      X=72 Y=0 Z=0
 8      X=84 Y=0 Z=0
 9      X=96 Y=0 Z=0
 10     X=108 Y=0 Z=0
 11     X=120 Y=0 Z=0
 12     X=132 Y=0 Z=0
 13     X=144 Y=0 Z=0
 14     X=0 Y=4 Z=0
 27     X=0 Y=8 Z=0
 40     X=0 Y=12 Z=0
 53     X=0 Y=16 Z=0
 66     X=0 Y=20 Z=0
 79     X=0 Y=24 Z=0
 92     X=0 Y=28 Z=0
 105    X=0 Y=32 Z=0
 118    X=0 Y=36 Z=0
 131    X=0 Y=40 Z=0
 144    X=0 Y=44 Z=0
 157    X=0 Y=48 Z=0
 1      X=0 Y=0 Z=0 F=1,12,12,1,13

SHELL
```

NM=1 O=0
1 E=1500 U=0.3 W=0.028935 M=0 TA=0
1 JQ=1,2,14,15 ETYPE=0 M=1 TZ=0 TH=5.125,5.125 LP=0 G=12,12

RESTRAINTS
157 157 1 R=1,1,1,1,0,1
144 144 1 R=1,1,1,1,0,1
131 131 1 R=1,1,1,1,0,1
118 118 1 R=1,1,1,1,0,1
105 105 1 R=1,1,1,1,0,1
92 92 1 R=1,1,1,1,0,1
79 79 1 R=1,1,1,1,0,1
66 66 1 R=1,1,1,1,0,1
53 53 1 R=1,1,1,1,0,1
40 40 1 R=1,1,1,1,0,1
27 27 1 R=1,1,1,1,0,1
14 14 1 R=1,1,1,1,0,1
1 1 1 R=1,1,1,1,0,1
169 169 1 R=0,1,1,1,0,1
156 156 1 R=0,1,1,1,0,1
143 143 1 R=0,1,1,1,0,1
130 130 1 R=0,1,1,1,0,1
117 117 1 R=0,1,1,1,0,1
104 104 1 R=0,1,1,1,0,1
91 91 1 R=0,1,1,1,0,1
78 78 1 R=0,1,1,1,0,1
65 65 1 R=0,1,1,1,0,1
52 52 1 R=0,1,1,1,0,1
39 39 1 R=0,1,1,1,0,1
26 26 1 R=0,1,1,1,0,1
13 13 1 R=0,1,1,1,0,1
161 161 1 R=0,1,1,1,0,1
148 148 1 R=0,1,1,1,0,1
135 135 1 R=0,1,1,1,0,1
122 122 1 R=0,1,1,1,0,1
109 109 1 R=0,1,1,1,0,1
96 96 1 R=0,1,1,1,0,1
83 83 1 R=0,1,1,1,0,1
70 70 1 R=0,1,1,1,0,1
57 57 1 R=0,1,1,1,0,1
44 44 1 R=0,1,1,1,0,1
31 31 1 R=0,1,1,1,0,1
18 18 1 R=0,1,1,1,0,1

```
5   5   1   R=0,1,1,1,0,1
165 165 1   R=0,1,1,1,0,1
152 152 1   R=0,1,1,1,0,1
139 139 1   R=0,1,1,1,0,1
126 126 1   R=0,1,1,1,0,1
113 113 1   R=0,1,1,1,0,1
100 100 1   R=0,1,1,1,0,1
87  87  1   R=0,1,1,1,0,1
74  74  1   R=0,1,1,1,0,1
61  61  1   R=0,1,1,1,0,1
48  48  1   R=0,1,1,1,0,1
35  35  1   R=0,1,1,1,0,1
22  22  1   R=0,1,1,1,0,1
9   9   1   R=0,1,1,1,0,1

LOADS
159 159 1   L=1 F=0,0,-0.5,0,0,0
146 146 1   L=1 F=0,0,-0.5,0,0,0
133 133 1   L=1 F=0,0,-0.5,0,0,0
120 120 1   L=1 F=0,0,-0.5,0,0,0
107 107 1   L=1 F=0,0,-0.5,0,0,0
94  94  1   L=1 F=0,0,-0.5,0,0,0
81  81  1   L=1 F=0,0,-0.5,0,0,0
68  68  1   L=1 F=0,0,-0.5,0,0,0
55  55  1   L=1 F=0,0,-0.5,0,0,0
42  42  1   L=1 F=0,0,-0.5,0,0,0
29  29  1   L=1 F=0,0,-0.5,0,0,0
16  16  1   L=1 F=0,0,-0.5,0,0,0
3   3   1   L=1 F=0,0,-0.5,0,0,0
167 167 1   L=1 F=0,0,-0.5,0,0,0
154 154 1   L=1 F=0,0,-0.5,0,0,0
141 141 1   L=1 F=0,0,-0.5,0,0,0
128 128 1   L=1 F=0,0,-0.5,0,0,0
115 115 1   L=1 F=0,0,-0.5,0,0,0
102 102 1   L=1 F=0,0,-0.5,0,0,0
89  89  1   L=1 F=0,0,-0.5,0,0,0
76  76  1   L=1 F=0,0,-0.5,0,0,0
63  63  1   L=1 F=0,0,-0.5,0,0,0
50  50  1   L=1 F=0,0,-0.5,0,0,0
37  37  1   L=1 F=0,0,-0.5,0,0,0
24  24  1   L=1 F=0,0,-0.5,0,0,0
11  11  1   L=1 F=0,0,-0.5,0,0,0
```

APPENDIX C
SAMPLE INTERPANEL DIFFERENTIAL DEFLECTION CALCULATION

This appendix contains a sample calculation of the interpanel differential deck deflection of a typical glulam girder bridge. The equations were developed in Chapter III.

1. Bridge Geometry and Loading

Center-of bearing to center-of-bearing span	94 ft
Bridge clear width	24 ft
Loading	AASHTO HS 20-44

2. Bridge girder and deck configuration

Girder size	12-1/4 in. wide by 64-1/2 in. deep
Deck size	5-1/8 in. thick by 48 in. wide
Center to center girder spacing	60 in.

3. Deck Material Properties

Deck panels are visually graded, southern yellow pine glued laminated panels conforming to specification symbol 24F-V4. Modulus of elasticity for the deck panels is 1,500,000 psi (AITC , 1993). Modulus of rigidity is assumed to be 1/16 of the modulus of elasticity.

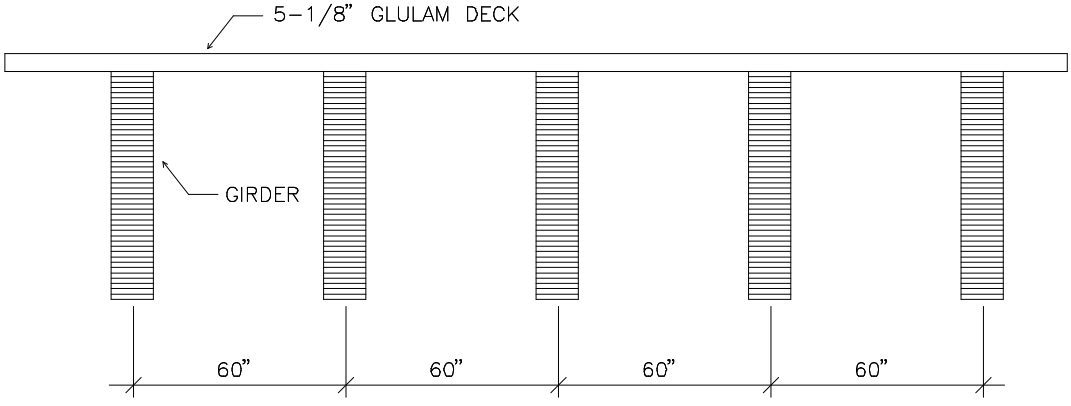

Cross Section of Bridge

4. Calculations

The moment of inertia for the deck is

$$I = \frac{bd^3}{12}$$ where b = deck panel width

$$I = \frac{(48in)(5.125in)^3}{12} = 538in^4$$

The expression for interpanel differential deflection is given by Equation 5.2.

$$y = \frac{1}{EI}\left(0.01621PL^3 + 0.12968d^2PL\right)$$

E = Modulus of Elasticity .....1,500,000 psi
I = Moment of Inertia .....538 in^4
P = AASHTO Wheel Load .....16,000 lbs
L = Span Length (girder to girder spacing) .....60 in
d = Deck Thickness .....5-1/8 in

Substituting the above values into the deflection equation

$$y = \frac{1}{EI}\left(0.01621PL^3 + 0.12968d^2PL\right)$$

$$y = \frac{0.01621(16{,}000lbs)(48in)^3 + 0.12968(5.125in)^2(16{,}000lbs)(48in)}{(1{,}500{,}000psi)(538in^4)}$$

$$y = 0.039 \ in$$

Since 0.039 in. is less than our allowable maximum deflection of 0.05 in., the design is adequate.

VITA

Joseph Neil Howard was born in Portsmouth, Ohio on February 27, 1956. He graduated with a Bachelor of Science Degree in Electrical Engineering from the University of Kentucky in 1983. He worked for Parrott, Ely and Hurt Consulting Engineers, Monongahela Power Company, and then became vice-president of Guyan Machinery Company. He earned his Master of Science degree in Civil Engineering in May 1997. Joseph N. Howard is currently pursuing a Ph.D. in Structural Engineering at Virginia Polytechnic Institute and State University.